91602
rev 83-10

COMPLIMENTARY COPY
Please Credit Ontario Hydro Research If
Reproduced in Whole or in Part

LEGAL NOTICE

This report was prepared by Ontario Hydro and, while effort has been made to assure the accuracy and applicability of the material contained herein, neither Ontario Hydro nor any person acting on its behalf:

(a) makes any warranty, express or implied with respect to the use of any information, apparatus, method or process disclosed in this report or that such use may not infringe privately owned rights; or

(b) assumes any liabilities with respect to the use of, or for damages resulting from the use of, any information, apparatus, method or process disclosed in this report.

ontario hydro
research division

METALLURGICAL INVESTIGATION OF CRACKING IN GENERATOR ROTOR SHAFT DARLINGTON NGS, UNIT 2

Report No. 91-7-K

M.A. Clark
Senior Engineer-Metallurgical
Metallurgy Section
Metallurgical Research Dept

ABSTRACT

Major cracks were discovered in the generator shaft in the vicinity of the radial holes containing the lead-in studs at the end of the generator windings. The investigaton has shown that the cracks initiated in a threaded section securing a nut used to retain the lead-in pin. Fretting between the two thread surfaces resulted in damage in the form of metal removal, distortion and microcracks. Under the influence of the bending stress generated by the rotor's own mass these microcracks changed orientation into the radial direction and grew to a critical size for fatigue crack growth. Propagation of the fatigue cracks continued in the radial plane due to the bending stress.

job	file	date	report no.
80-136-552	823.428	February 18, 1991	91-7-K

91602
new 82-10

92-00874/

ontario hydro
research division

EXECUTIVE SUMMARY

METALLURGICAL INVESTIGATION OF CRACKING IN GENERATOR ROTOR SHAFT, DARLINGTON NGS, UNIT 2

M.A. Clark

In March of 1990, large cracks were discovered in the main shaft of the Darlington U2 generator. The Darlington turbine-generators are 935 MW units operating at a speed of 1800 RPM. The generator is a four pole design and is constructed from a low alloy steel forging of material specified by the manufacturer with a nominal composition of: 3.5% nickel, 1.5% chromium, 0.5% molybdenum, 0.1% vanadium and 0.25% carbon. The unit was first started, at low speed, on January 6 1990 with first run up to 1800 rpm occurring on January 8. The unit ran with some interruptions until increased generator bearing vibrations were detected on March 7 and the unit removed from service on March 8. At that time the generator had run for approximately 841 hours at 1800 rpm and had experienced a total of 5 overspeed excursions.

Early NDE visual inspection detected a large crack in the rotor shaft which appeared to originate in a lead-in stud hole. The shaft contains four radial holes which penetrate the shaft to the central bore hole and contain the copper lead-in and throughout studs. The studs are held in the holes by steel retaining nuts threaded into the shaft at a location recessed below the outer surface of the shaft.

This report covers the metallurgical investigation, conducted by Ontario Hydro Research, into the nature and cause of the cracking.

The investigation consisted of four main steps; replica examination of the cracks in the U2 rotor before the cracks were broken open, examination of one half of a retaining nut from the Unit 4 rotor, analysis of one half of the fractures from the U2 rotor after the shaft was broken open and determination of chemical and mechanical properties. The investigation has shown that the measured properties of the rotor material were all normal and were within or exceeded all specifications. Fretting damage in the form of metal removal, distortion and microcracks was found on the retaining nut and shaft thread surfaces in the lead-in stud hole.

job	file	date	report no.
80-136-552	823.428	February 18, 1991	91-7-K

This fretting has been produced by a combination of centrifugal loads on the stud pins and flexing of the shaft from bending stresses. The fretting damage progressed into microcracks which became oriented into the radial planes under the influence of the bending stress generated by the rotor's mass. These microcracks provided the initiating sites for the propagation of fatigue cracks driven by the same alternating bending stresses. Some evidence was found that environmental hydrogen assisted in the fatigue crack propagation.

TABLE OF CONTENTS

1.0	INTRODUCTION		1
2.0	METALLURGICAL INVESTIGATION		2
	2.1 Replica Examination		3
	2.2 Retaining Nut Examination		3
	2.3 Shaft Fracture Examination		4
	2.3.1	Methods	4
	2.3.2	Visual Examination, as broken	5
	2.3.3	Visual Examination, as cleaned	5
	2.3.4	Fractography, small crack	5
	2.3.5	Metallography, small crack	6
	2.3.6	Metallography, threads	7
	2.3.7	Fractography and Metallography, secondary cracks	8
	2.3.8	Fractography and Metallography, large crack	9
	2.4 Mechanical and Chemical Properties		10
3.0	DISCUSSION		10
4.0	CONCLUSIONS		11
5.0	ACKNOWLEDGEMENTS		12

LIST OF FIGURES

Figure 1	Generator Rotor Design	13
Figure 2	Cross Section of Lead-In Stud Hole	14
Figire 3	Pole 1 Region, Unit 2	15
Figure 4	Details of Large Crack In Pole 1 Region	16
Figure 5	Details of Small Crack In Pole 1 Region	17
Figure 6	Details of Cracking From Replicas, Pole 1, Unit 2	18
Figure 7	Retaining Nut, Unit 4	19
Figure 8	Cross Section of Nut	19
Figure 9	Detail of 4th Thread From Top	20
Figure 10	Surface of Thread 3	20
Figure 11	Cross Section of Thread 4	21
Figure 12	Cross Section of Thread 7	21
Figure 13	View of Thread Surfaces	22
Figure 14	General Appearance of Shaft	23
Figure 15	Details of Large Crack	24
Figure 16	Details of Small Crack	25
Figure 17	Schematic of Shaft Section	26
Figure 18	General Appearance of Crack Surfaces	27
Figure 19	Details of Large Crack	28
Figure 20	Details of Small Crack	29
Figure 21	Details of Initiation Region and Thread Numbering	30
Figure 22	Fretting Damage to Thread 1 Adjacent to Fracture	31

Figure 23	Lower Face of Thread 2 Adjacent to Fracture	32
Figure 24	Upper Face of Thread 2 Adjacent to Fracture	33
Figure 25	Fracture Surface, Small Crack, Threads 1-6	34
Figure 26	Fracture Surface, Small Crack, Thread 1	35
Figure 27	Fracture Surface, Small Crack, Thread 2	36
Figure 28	Fracture Surface, Small Crack, Propagation Zone	37
Figure 29	Metallography of Small Crack	38
Figure 30	Microstructure of Small Crack	39
Figure 31	Location of Metallographic Sections, Small Crack	40
Figure 32	Microstructure of Thread Root #1, Small Crack	41
Figure 33	Details of Fretting Damage, Thread Flanks	42
Figure 34	Microstructure of Thread #6, Small Crack	43
Figure 35	Typical Fretting Microcracks	44
Figure 36	Fretting Damage Behind Small Crack	45
Figure 37	Development of Cracks From Fretting Damage	46
Figure 38	Fine Fretting Cracks	47
Figure 39	Location of Secondary Crack Behind Small Crack	48
Figure 40	Location and Microstructure of Secondary Crack	49
Figure 41	Details of Crack Path of Secondary Crack	50
Figure 42	Fractography of Secondary Crack	51
Figure 43	Initiation Region of Secondary Crack	52
Figure 44	Fractographic Details of Secondary Crack	53
Figure 45	Fractography of Secondary Crack, ABB	54

Figure 46	Detailed Fractography	55
Figure 47	Detailed Fractography	56
Figure 48	General Appearance of Initiation Zone of Large Crack	57
Figure 49	Fracture Surfaces, Threads 1-3, Large Crack	58
Figure 50	Fracture Surfaces, Threads 4 and 6, Initiation Zone	59
Figure 51	Details of Initiation Zone, Thread 6, Large Crack	60
Figure 52	Metallography of Thread Surfaces Behind Large Crack	61
Figure 53	Metallography of Large Crack, Fracture Plane and Thread Surface, Thread 6	62
Figure 54	Absorbed Energy vs Temperature - U2 Generator Shaft	63
Figure 55	Lateral Expansion vs Temperature - U2 Generator Shaft	64
Figure 56	Fracture Appearance vs Temperature - U2 Generator Shaft	65

LIST OF TABLES

		PAGE
TABLE 1	Results of Chemical Analysis Unit 2, Generator Shaft	66
TABLE 2	Tensile Properties of Rotor Steel	67

ontario hydro
research division

TO Mr. M.A. Machacek
Manager of Engineering
Darlington Engineering

METALLURGICAL INVESTIGATION OF CRACKING IN GENERATOR ROTOR SHAFT, DARLINGTON NGS, UNIT 2

M.A. Clark

1. INTRODUCTION

In March of 1990, abnormal vibration levels were detected in the Darlington Unit 2 generator shaft bearings. The unit was taken out of service for inspection and large cracks were discovered in the main generator shaft. This report covers the metallurgical investigation, conducted by Ontario Hydro Research, into the nature and cause of the cracking. A parallel investigation has been conducted by the generator manufacturer(ABB).

The Darlington turbine-generators are 935 MW units operating at a speed of 1800 RPM. The generator is a four pole design and is constructed from a low alloy steel forging of material specified by the manufacturer with a nominal composition of: 3.5% nickel, 1.5% chromium, 0.5% molybdenum, 0.1% vanadium and 0.25% carbon.

In the area of the cracking the shaft diameter was 875 mm. The original tendered design had called for a diameter of 1100 mm but this had been reduced to alter the critical speeds of the rotor as the original 2nd critical speed was close to operating speed. This reduction in diameter resulted in a 100% increase in nominal bending stress at the crack location.

The following is a summary of the operating history of the Unit 2 turbine-generator from January 6 to March 8, 1990. The unit was first started, at low speed, on January 6 1990 with first run up to 1800 rpm (operating speed) occurring on January 8. One overspeed test was performed at that time. The unit then ran for approximately 10 days at operating speed until a turbine outage was taken from January 19-Feb 7. After restart a second overspeed test was performed then the unit run for several days until a power failure test on Feb 16 which resulted in another overspeed to 1818 rpm. On restart on Feb 17, some abnormal bearing vibrations were noted. The generator then ran at steadily increasing load levels until 414 MW was reached on March 2. Two turbine load rejection tests producing turbine overspeeds were performed on March 3 followed by a

brief outage. High vibrations were again noted on startup but not at 1800 rpm. Increased generator bearing vibrations were detected on March 7 and the unit removed from service on March 8. At that time the generator had run for approximately 841 hours at 1800 rpm and had experienced a total of 5 overspeed excursions.

Early NDE visual inspection detected a large crack in the rotor shaft which appeared to originate in a lead-in stud hole. Details of the rotor design in this vicinity are shown in Figure 1 and the details of the lead-in stud hole shown in Figure 2. In this area the shaft contains four radial holes which penetrate the shaft to the central bore hole. When assembled these holes contain the copper lead-in and throughout studs. The studs are held in the holes by steel retaining nuts (Figure 2) threaded into the shaft at a location recessed below the outer surface of the shaft.

Two cracks were detected in one of the lead-in stud holes (Pole 1) and appeared to originate from the general region of the threaded section containing the retaining nut. Figure 3 shows the Pole 1 hole with the stud removed. The larger of the two cracks had progressed out of the hole onto the outer surface of the shaft and around the shaft in a circumferential direction about 400 mm (Figure 4). It had also progressed downward into the hole through the retaining nut threads and towards the shaft bore. The smaller crack was on the other side of stud hole almost opposite the larger crack (Figure 5). It had not progressed onto the outer surface of the shaft but appeared to be centred on the threaded region.

2. METALLURGICAL INVESTIGATION

The Ontario Hydro metallurgical investigation into the cause of the rotor cracking consisted of four main steps;

1) replica examination of the cracks in the U2 rotor before the cracks were broken open

2) examination of one half of a retaining nut from the Unit 4 rotor.

3) fracture examination of one half of the fractures from the U2 rotor after the shaft was broken to reveal the cracks.

4) determination of chemical and mechanical properties.

The report will present the results of these investigations in the same order.

It was postulated by the manufacturer early in the investigation that the cracking was caused essentially by fatigue induced by high bending stresses but was initiated by fretting between the retaining nut and the threaded portion of the shaft. The first two steps listed above were attempts to provide early information relevant to these postulated mechanisms.

2.1 REPLICA EXAMINATION

The initial replica examination was carried out on the U2 and U4 rotors on site at Darlington. It consisted of acetate and rubber replicas of selected sites in the stud holes and shaft surfaces.

The rubber replicas were taken of the retaining threads in the shaft to provide a record of the thread condition and for examination for fretting. The acetate replicas taken after metallographic polishing were intended to reveal the crack features and the material's microstructure. Location of the acetate replicas are shown in Figure 4 (indicated by arrows). Details of the cracks as seen on the replicas are shown in Figure 6.

The cracks were seen to be straight, transgranular and not branched all of which are general features of fatigue cracks in this material. The general microstructure consisted of tempered bainite and no manufacturing defects were detected on the areas covered by the replicas.

The rubber replicas did detect the presence of fretting damage on the thread flanks most notably on the under side of the thread surfaces in the rotor. Since details of the fretting damage on the actual threads will be presented in detail later no further discussion of rubber replicas is needed at this point. The tentative conclusions drawn from the replica examinations were that the features were characteristic of fatigue cracking and that thread fretting damage was present.

2.2 RETAINING NUT EXAMINATION

One half of the retaining nut from the Unit 4 rotor was examined for early signs of fretting damage. The as-received appearance of the nut and a cross section through the threads are shown in Figures 7 and 8. Portions were cut from each end of the sample and examined in the scanning electron microscope(SEM). The typical appearance of the thread surfaces are illustrated in Figure 9. In all cases the threads are numbered from the top surface(surface towards the shaft outer diameter when installed in the rotor). The top surfaces of each thread displayed evidence of fretting wear of varying degrees. The bottom surfaces of each thread displayed either no damage or less damage than the corresponding top surface. A typical fretted surface is shown in Figure 10 and contrasted to the original machined surface at the end of the contact zone in the right hand view.

In metallographic cross section, the fretting was generally manifested as distortion of the grain structure in shallow surface layers (Figure 11). In some cases extrusion of the surface layers was present at the end of the thread contacts (Fig. 11, right). The severity of the fretting appeared to generally increase from the top threads towards the bottom (Figure 13). The most distorted threads were #7 and 8. A cross section of thread #7 is seen in Figure 12. It is felt that this distortion is so severe that it was not due just to fretting but was partially produced on removal of the nut from the shaft. It was reported that this nut was particularly hard to remove. In summary, the U4 retaining nut examination showed that:

· fretting damage was present on the retaining nut contact surfaces

. this damage was more severe on the top (outer) surfaces of the thread flanks

. the damage got progressively worse from the outer threads to the inner.

2.3 SHAFT FRACTURE EXAMINATION

After all NDE inspection was completed on the Unit 2 rotor cracks, the shaft was fractured to reveal the crack surfaces. This was accomplished by sawing large wedges from the rotor in locations directly opposite the cracks and then fracturing the remaining ligaments by applying bending forces to the end of the rotor at the exciter end. The exciter end portion of the fracture was examined by ABB; the other half was made available to Ontario Hydro and was used for the present investigation and to supply material for a fatigue and fracture property investigation conducted by the Fracture Technology Section of OHR.

2.3.1 METHODS

After receipt of the shaft, the metallurgical investigation consisted of the following components:

Visual examination
Cleaning of fracture surfaces
Cutting
- .removal of fracture surfaces
- .samples for fatigue testing
- .samples for mechanical testing

Further cleaning of fractures
Fractography
Metallography
Chemical analysis
Tensile, impact and hardness testing.

The cleaning of the fractures was necessary because an oil-based solution was injected into the crack as part of an eddy current examination before the shaft was fractured. After fracture this oil obscured many of the fracture features. It proved very difficult to remove. Initial cleaning was attempted in soap-water solutions, varsol, acetone, trichloroethane and by application of acetate tape to mechanically strip the deposit. None were completely successful but some removal was achieved by the use of trichloroethane in an ultrasonic bath. For detailed fractography some fracture areas were chemically cleaned in an hydrochloric acid solution containing dibutyl thiourea(DBT).

2.3.2 VISUAL EXAMINATION, as broken

The appearance of the shaft immediately after cutting is shown in the series of Figures 14 through 16. The majority of the large crack, to right of Fig.14, was covered with the black deposit from the oil. Only the extremities of the crack had the dull colour typical of fresh fractures. Part of the large crack was also missing, being contained in the wedge cutouts. Little detail of the large crack could be seen through the deposits except for two prominent ridges or beach marks which started just above the shoulder containing the threads(Figure 15). These marks provide some indication that the crack had initiated somewhere in the threaded region. The remainder of the fracture face was flat and featureless except for another prominent beach mark at the crack extremity close to the outer shaft surface.

As suspected, the small crack did not extend much beyond the threaded shoulder region in the outward direction but had grown downward towards the bore a somewhat greater distance(Figure 16). Again the fracture face in the threaded region was obscured, but the pronounced beach marks were not apparent. The general shape of the crack however also indicated initiation in the threads. In the thread region several fine ridges were seen emanating from the threads. The unobscured fracture face was a dull grey colour and had some faint ridges. A light grey band of smoother surface was apparent around the crack extremity.

The dimensions of the shaft supplied to OHR and the approximate relative areas of the two cracks are shown in the schematic of Figure 17.

2.3.3 VISUAL EXAMINATION, as cleaned

After the attempts to remove the oily deposits, the fractures were again examined visually(Figure 18). Traces of the oil remained since it appeared to have reacted with the fracture surfaces so that the initial oxide layers on the fracture had been altered in some way. The two beach marks in the shoulder region of the large crack could still be seen but were less prominent (Figure 19). On the small crack surface, the small ridges could still be clearly seen (Figure 20). These ridges are usually termed 'ratchet marks' and are associated with multiple simultaneous crack initiation sites which ultimately grow together to form a single crack.

Since the small crack was apparently less affected by the surface contamination and had more interesting features in the initiation region, it was examined initially and ultimately in more detail. The results of the fractography and metallography of the small crack will be presented first.

2.3.4 FRACTOGRAPHY, small crack

The crack surface in the region of the upper threads is shown in Figure 21. The threads are numbered from the thread closest to the outer rim of the shaft as shown. The ridges were associated with the first five threads, the rest of the fracture being relatively smooth. The general pattern of the ridges and the fracture surface indicated that the initiation point was from the under side of each thread. This would be the side loaded by the corresponding retaining nut threads responding to centrifugal forces on the stud. The flanks of the threads adjacent to the fracture

were examined in the SEM. In Figure 22 the specimen is tilted away from the fracture surface(dark region to right) so that the flanks can be seen as well. The fretting damage on the thread is seen to the upper left and the end of the contact zone is shown in more detail in the lower view. A similar pattern to that of the retaining nut was seen in all threads; the lower, loaded side contained the fretting damage while the upper side was virtually undamaged(Figure 23).

The investigation of the fracture faces was hampered considerably by the contamination but also by post fracture damage to the surface. Some of the threads were severely damaged during the removal process(Figure 24) but more importantly rubbing together of the crack surfaces during operation followed by some oxidation had destroyed many of the fine fracture features. This was particularly true in the initiation regions. However, examination of the fracture showed that, in general, the features in the upper threads were indicative of initiation from the fretted side of the thread flanks. Small flat regions on each thread were found more or less centred on the loaded side of the threads(Figure 25). In thread 1 traces of a fine beach mark could be seen with the end of the contact zone at its approximate centre(Fig 25a). The remains of river pattern marks could also be seen (Fig 25b). Both of these features point to initiation from the end of the contact region. The end of the ridge can be seen as a step joining two of these flat initiation regions in adjacent threads(Fig25a). In other threads the initiation was not as well indicated,for instance in thread 2, the beach mark and the fine ridges were not obvious(Figure 26). What pattern did exist indicated possible initiation higher up towards the tip of the thread(Fig 26b).

Away from the initiation region the features of the cracking were again obscured. The general appearance is shown in Figure 28a. Occasional traces of possible fatigue striations could be found (centre of Fig 28a). At the tip of the small crack about 6 cm from the threads the fracture surfaces were relatively clean and the fracture mode was distinctly different with a predominately faceted intergranular appearance(Fig 28b).

2.3.5 METALLOGRAPHY, small crack

After fractographic examination, the small crack was sectioned and prepared metallographically in a plane through the 4-5 thread root at right angles to the main fracture plane. The results are shown in Figures 29 and 30. In Figure 29 a), the main fracture plane is horizontal and the thread root surface vertical. The fracture plane had a slight curvature at this location but was generally flat. A few branches were found from the main crack; one is shown in Figure 29 b) which contains a portion of the main and branch crack. The branch crack provided some information on the nature of the crack path whereas the main crack did not because of the rubbing damage resulting from contact of the fracture faces(Fig 30 a and b). In the branch crack the path was partially intergranular as indicated by the flat facets. This could be significant to the failure mode since intergranular cracking in this material could be produced by the influence of hydrogen. This will be discussed in more detail later. The general microstructure of the material in all of the sections examined consisted of tempered bainite; an example is shown in Fig 30c.

2.3.6 METALLOGRAPHY, threads

To obtain information about the fretting damage on the threads, metallographic sections were taken in planes behind and parallel to the fracture plane (Figure 31). Details of the damage found on the thread flanks are presented in Figures 32 through 33. A general view of the thread root area is shown in Figure 32 and illustrates the area at the end of the contact zone. This is seen in more detail in Figure 33 a) where extrusion of the metal is apparent. This form of the damage is similar to that seen in the retaining nut(see Figure 11). Higher up the thread flank more severe damage was typically found (Fig 33 b). In this case a large shallow pit or gouge could be seen together with a microcrack. A more severe example is shown in Figure 34. Many of these microcracks were found on the cross sections; some typical examples are seen in Figure 35. These cracks had a depth of about 0.1 - 0.2 mm and were generally oriented at an angle of about 45° to the surface. This suggests that they are formed by shear stresses generated by the thread contact forces.

Further information about the fretting marks and their relationship to the crack initiation was obtained by sectioning in planes orthogonal to those of Figure 31 in the area immediately behind the main fracture. Location and viewing direction are indicated in the top insert of Figure 36. Pertinent results are shown in Figure 36; these results are either from the second or third threads. The main fracture face is always to the right of each figure and indicated by arrows. A series of sharp bottomed, wide mouthed projections could be seen on the first section. The orientation of these features roughly paralleled the angle of the main crack at the initiation point. At higher magnifications, many of the wide projections contained fine cracks at their apex (Fig 36a). At lower levels in the threads numerous fine cracks were also found but not necessarily associated with the wide projections (Fig 36b). About the middle of the thread profile (section 4) the wide projections were no longer present but the fine cracks remained. In all sections the microcracks were oriented at 45° close to the surface then gradually changed to about 90° as they progressed. The main fracture path followed the same pattern.

The wide part of the cracks were filled with a deposit (Figure 37). Energy dispersive X-ray analysis(EDXA) of the deposits showed them to contain mostly Fe with lesser but significant amounts of Si,S,Cr,Ni, and Zn. Most of these elements would be expected from oxidation of the shaft steel except for the S and Zn. The sulphur could come from anti-sieze compounds such as molybdenum disulphide, if they had been applied to the nut. The Zn would not normally be expected but the retaining nut was zinc plated. Thus the presence of Zn in these cracks indicates transference of material from the nut to the shaft surfaces by the fretting mechanism and hence provides supportive evidence for the fretting origin. The appearance of one of the deposit filled projections and associated microcracks is illustrated in Figure 37.

On the fifth section, most of the these features had disappeared except for some fine microcracks. At high magnifications, these cracks displayed the same change in orientation of the larger cracks; starting initially at 45° then changing to a more orthogonal orientation (Figure 38). Most were obviously initiating in the surface layers which were undergoing deformation from the fretting. This is particularly true in the top view of Figure 38 where grain deformation can be seen around the crack at the surface. The microcracks at he the initiation point were not always

inclined in the same direction as the main crack; this is illustrated by comparing the top and bottom views of Figure 38. Thus it would appear that the microcracks develop at the surface under the local shear stress and as they grow come under the influence of the overall bending stress and change orientation into the axial plane of the main crack. The wide mouth of the cracks probably is developed later as the cracks grow and the surfaces oxidize.

2.3.7 FRACTOGRAPHY AND METALLOGRAPHY, secondary cracks

During the initial SEM examination of the thread surfaces. a small secondary crack was discovered immediately behind and parallel to the main fracture plane of the small crack. Its location and orientation are shown in Figure 39 which is a view of the fretted thread flanks of thread 4. The secondary crack appeared to extend only from the root between thread 4 and 5 and across the tip of thread 4. Since it was oriented parallel to the main crack and appeared to originate in the fretted region, its fracture mechanism was probably the same as the main crack and hence it could provide valuable information in the overall crack mechanism. Therefore it was subjected to metallographic examination in a plane through the root between 4-5 threads, then broken open to reveal the fracture features.

The metallographic observations are summarized by Figure 40. The secondary crack path was exactly parallel to that of the main crack for the length visible in this view. The fracture path again appeared to be a mixture of transgranular and intergranular mode (Figure 40b). The high magnification SEM views in Figure 41 illustrate this feature.

After examining the metallographic sections, the secondary crack was broken open to reveal the general pattern of Figure 42. Two distinct zones were evident: a light coloured initiation zone extending over the thread profile and part way below the thread root and a darker zone extending into the bulk of the shaft(Fig 42a). The crack appeared to have extended slightly beyond the cutting planes used to open the crack. The beach markings and the ridge patterns clearly indicated the origin of this crack to be darker regions along the fretted side of the thread flank. In fact, the exact initiation site was the somewhat darker oxidized region close to the tip of the thread (Fig 42b). Closer examination of this region (Figure 43) showed that on one half of the fracture there was a depression which matched a projection on the other half. Thus the initiation site was inclined at an angle to the main fracture plane. It was thus in all probability one of the wide mouth fretting cracks similar to that seen in Figure 36. Details of the fractographic features in the secondary crack are seen in Figure 44. Rubbing damage between the fracture faces was not apparent and details of the crack propagation were much clearer than on the main cracks. The initiation region was covered with a deposit (seen in upper part of Figure 44a). The remainder of the fracture was somewhat cleaner and a finely ridged pattern was seen in both the initial propagation regions and in the regions close to the extremity of the crack. Some isolated regions of faceted intergranular fracture were seen but were not a general feature of the surface(Fig 44b) . A light oxide covering prevented the examination of actual fatigue striations. Assuming all of the the dark region along the thread flank in Figure 42b to be the initiating crack for fatigue crack propagation, the nominal critical crack size was then 1.5mm in length and 0.2mm in depth.

A similar but somewhat smaller secondary crack was discovered by ABB and was made available for our examination. The results of the examination were very similar to the above and are presented in Figure 45-47. Again the general ridge pattern pointed to initiation in a darker region towards the tip of the thread. The flank of the thread was not intact since ABB had sectioned in a plane(right of Fig 45a) through this region. This crack had only extended to the depth of the thread. Fractographic features were very similar to those of the other secondary crack(Figure 46); a finely ridged,transgranular pattern. However at very high magnifications (figure 47), traces of possible fatigue striations could be seen particularly in the middle of the propagation zone (Fig 47a). Attempts were made to calculate the spacing of the striations and determine a crack propagation rate: a rate of about 2×10^{-7} m/cycle was estimated at a location corresponding to a crack length of 0.7 mm. It should be noted that fracture surfaces of the laboratory fatigue tests on the rotor material did not display striations.

2.3.8 FRACTOGRAPHY AND METALLOGRAPHY, large crack

The main large crack was also subjected to the same type of examinations but rubbing damage, oxidation and oil contamination were all more severe so that fractographic information was less clear than the other cracks.

The general appearance of a portion of the main crack is again presented in Figure 48; taken after the final attempts to clean the surface. The two distinct beach marks mentioned previously were still present. It was noted that they are of the same shape and size as the extremity of the small crack (see Fig. 20). In contrast the small crack, the ridges or ratchet marks were not obvious except for perhaps one in the region of the 7th thread.

Upon examination of the thread regions in the SEM, similar features to the small crack were seen (Figure 49). The surfaces were mostly flat; the general ridge pattern again pointed to multiple origins on the undersides of the thread flanks. Two of these origins are seen in Figure 50. The 6th thread fracture surface contained some interesting features; two small smooth zones on the thread flank about mid way down the thread side which appeared very similar to the fretting cracks as seen on the secondary cracks (Figs 42 and 45). The higher magnification views of Figure 51 confirmed the similarity to the secondary crack features and in addition a small fretting crack was found in the immediate vicinity (Fig 51b). Similar fretting microcracks were found on thread cross sections immediately behind the main cracks (Figure 52). Sectioning in orthogonal planes to the fracture planes also revealed fretting damage and a direct link of the main fracture to the fretting microcracks (Figure 53). These are sections through the area of thread #6 shown in Fig 51 and show both the fracture plane and a portion of the thread flank surface (Fig 53). Numerous fretting microcracks were found along the thread surface; most were at 45° but some were reoriented to 90°. A small projection at the apex of the fracture and thread planes was the initiation point and probably corresponds to the smooth area of Fig. 51a. The microcracks across the apex joining the two surfaces obviously originate as fretting microcracks.

Thus it has been shown that the features of cracking in the main large crack are generally the same as that in the small crack and in the two secondary cracks: numerous fretting microcracks on the thread flanks, initiation of the fatigue cracks from the microcracks, propagation of the fatigue cracks by a mixed transgranular and intergranular mode.

2.4 MECHANICAL AND CHEMICAL PROPERTIES

The mechanical and chemical properties of the shaft material were determined in the rim, mid radius and bore positions by taking samples from the OH fracture half of the shaft.

The results of the chemical analysis are presented in Table 1 and compared to the manufacturer's specified values. In all of the major specified alloying elements, the measured concentrations were within the specified ranges, In addition, there was little variation in these concentrations with radial position in the shaft. All of the minor trace and impurity elements which can influence fracture properties were at low and acceptable values. Similarly all of the tensile properties exceeded the specified values (Table 2). Some slight reduction in UTS and yield strength was found from the rim to the bore position. This is not unexpected in a forging of this size.

The impact properties were measured in two locations, rim and bore, utilizing standard Charpy V-notch specimens. Typical absorbed energy, lateral expansion and percent shear vs test temperature curves are presented as Figures 54-56. $FATT_{50}$ values of -52°C and -26°C were found at the rim and bore locations respectively. Again the impact properties are what would be expected from a steel of this type and should not have been a factor in the failure.

3. DISCUSSION

The metallurgical investigation of the retaining nut and the cracked shaft has provided support to the original postulated mechanism of fatigue cracking initiated by fretting between the thread surfaces. Fretting damage was found on the threads of the retaining nut from Unit 4 despite the fact the rotor had only experienced a few rotational bending cycles. Similar appearing damage was found in the shaft threads in the Unit 2 rotor. The fretting was most severe on the top of the thread flanks in the nut and the bottom flanks in the shaft. The contact stresses on the threads was therefore due to the centrifugal forces acting on the studs in conjunction with the flexing of the shaft due to the bending stresses. The pole pin and the retaining nut would be relatively rigid compared to the shaft.

The fretting damage took several forms; metal removal and gouging, local deformation and microcracking. The most serious form in regard to fatigue crack initiation was the microcracking. In the early stage of development the microcracking was generally oriented locally at 45° to the surface. When the microcracks were in the location of the maximum bending stress they gradually changed orientation to that of the main radial fracture plane. When these re-oriented microcracks reach a certain critical size they grow by a high cycle fatigue mechanism driven by the alternating bending stresses.

The main fatigue cracks initiated at several threads simultaneously because the general nature of the fretting damage provided numerous microcrack sites. The very small critical size for the onset of fatigue crack propagation (about 1 mm.) provides evidence that the bending stresses were very high in the thread area. High stress concentrations would be expected because of the radial holes and the threads. As stated above, the nominal bending stresses were higher than the original design because of design changes.

Because of post crack rubbing , oxidation and contamination of the main fracture plane, little evidence of fatigue striations was found hence detailed information on crack growth rates was not obtained. Only one area on a secondary crack had some faint striation-like markings and a crack growth rate of 2×10^{-7} m/cycle was estimated. However, there was some evidence that the hydrogen environment in the generator may have been influencing the fatigue crack propagation. Intergranular facets were found in several areas of the main cracks particularly in the later stages of propagation but some were found very close to the initiation region. Metallographic evidence for a partial intergranular crack path was also found in several areas most notably in one of the secondary cracks behind the main cracks(Figure 40).

Intergranular crack paths can be produced in this material under a variety of conditions: dynamic loadings when the steel has been temper embrittled, static loadings in environments causing stress corrosion cracking particularly those producing absorbed hydrogen. In fatigue conditions there is also evidence that the effect of hydrogen is to produce an intergranular crack path and perhaps coincidently to increase the fatigue crack propagation rates. In one study/1/ using a similar NiCrMoV steel no intergranular facets were found at any stress intensity when tested in air but were produced in hydrogen but only at intermediate stress intensities. The laboratory fatigue test program at OH has discovered evidence of intergranular fracture mode in this material when tested in hydrogen but not in air so far. On the other hand, ABB's fatigue test program has produced intergranular fracture modes in air at certain stress intensities. The issue obviously requires further investigation. However the occurrence of the intergranular mode in several areas of the fracture surface and thus at a range of stress intensities does suggest hydrogen was influencing the behaviour. Hence, at this point, only fatigue data generated in hydrogen should be used in future calculations of crack initiation sizes and growth rates.

4. CONCLUSIONS

1. The measured properties of the rotor material were all normal and were within or exceeded all specifications.

2. Fretting damage was present on the retaining nut and shaft thread surfaces in the lead-in stud hole. This fretting has been produced by a combination of centrifugal loads on the stud pins and flexing of the shaft from bending stresses.

3. The fretting damage progressed into microcracks which became oriented into the radial planes under the influence of the bending stress and provided the initiating sites for the propagation of fatigue cracks.

4. The majority of the crack area was produced by a bending fatigue mechanism.

5. Some evidence was found that environmental hydrogen assisted in the fatigue crack propagation.

5. ACKNOWLEDGEMENTS

The author wishes to thank the following members of the Metallurgical Research for their contributions to this investigation: Mr. A. Cervoni and Mr. S. Nixon for field investigations, lab metallography and mechanical testing, D. Limoge for lab metallography and SEM analysis, Mr. F. Smith for SEM analysis, and Ms. Cheng Min for metallography.

Recommended by:

W.H.S. Lawson
Supervising Engineer
Metallurgy Section
Metallurgical Research Dept

Prepared by:

M. A. Clark
Senior Metallurgical Engineer
Metallurgy Section
Metallurgical Research Dept

Approved by:

Brown
Manager
Metallurgical Research Dept

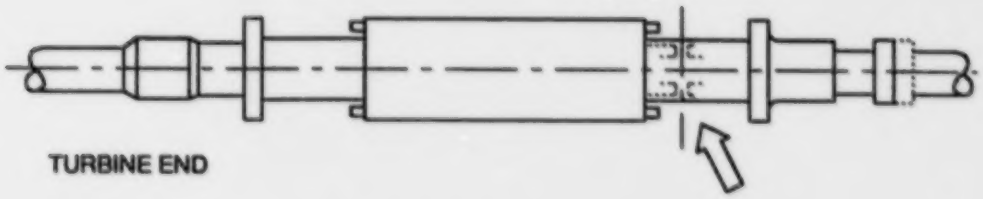

a) Schematic of Generator Rotor

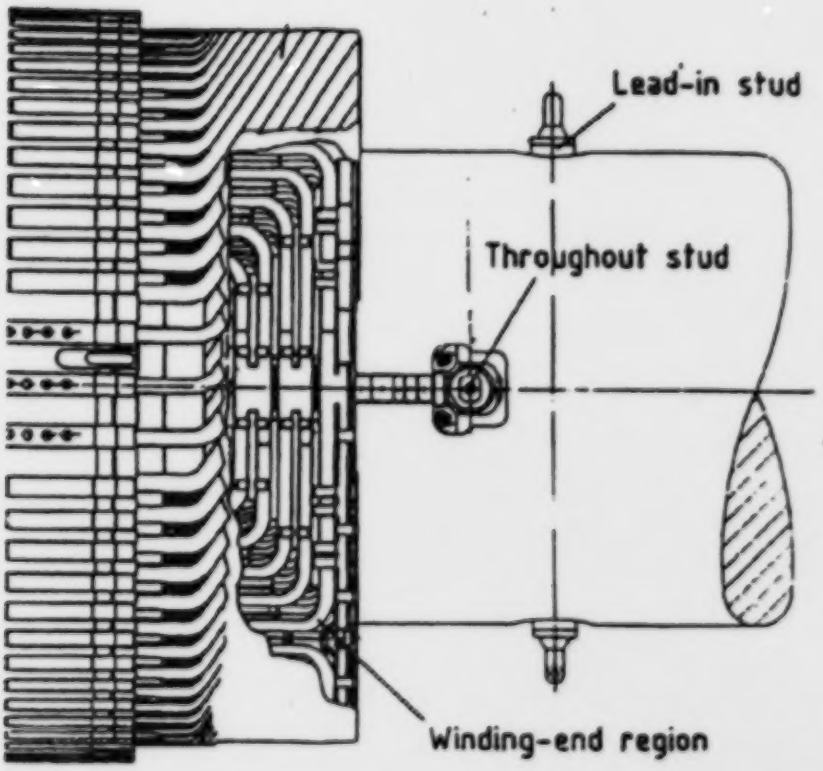

b) Detail of Rotor at Crack Location

FIGURE 1

GENERATOR ROTOR DESIGN

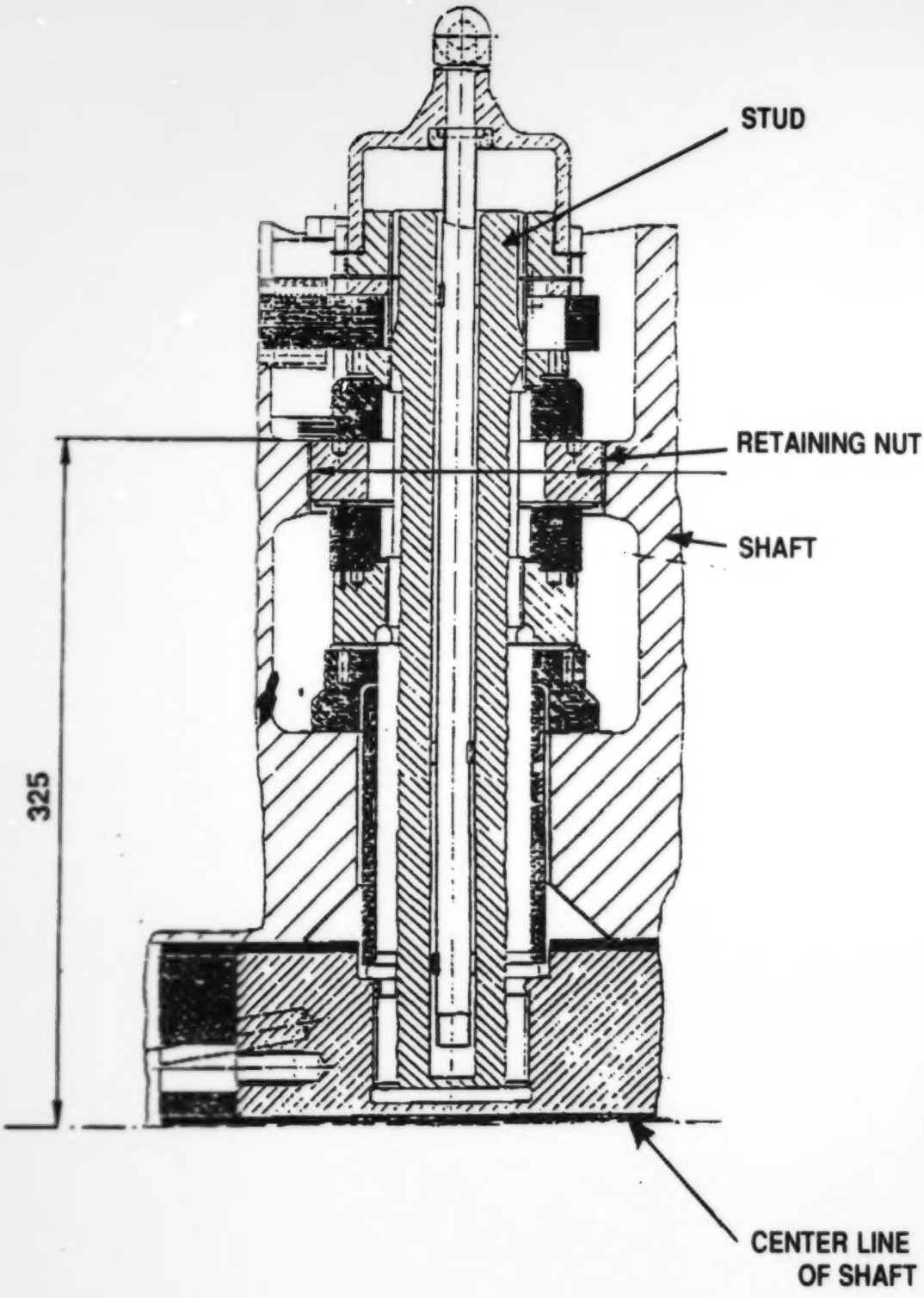

FIGURE 2 - CROSS SECTION OF LEAD-IN STUD HOLE

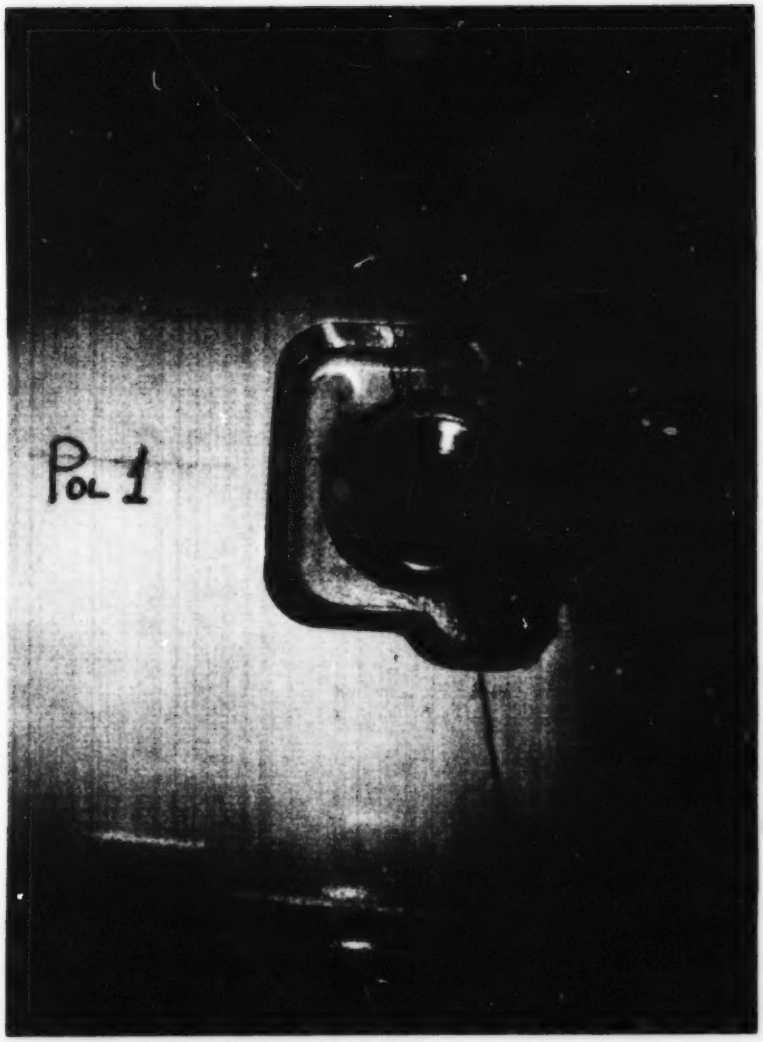

FIGURE 3 - POLE 1 REGION, UNIT 2

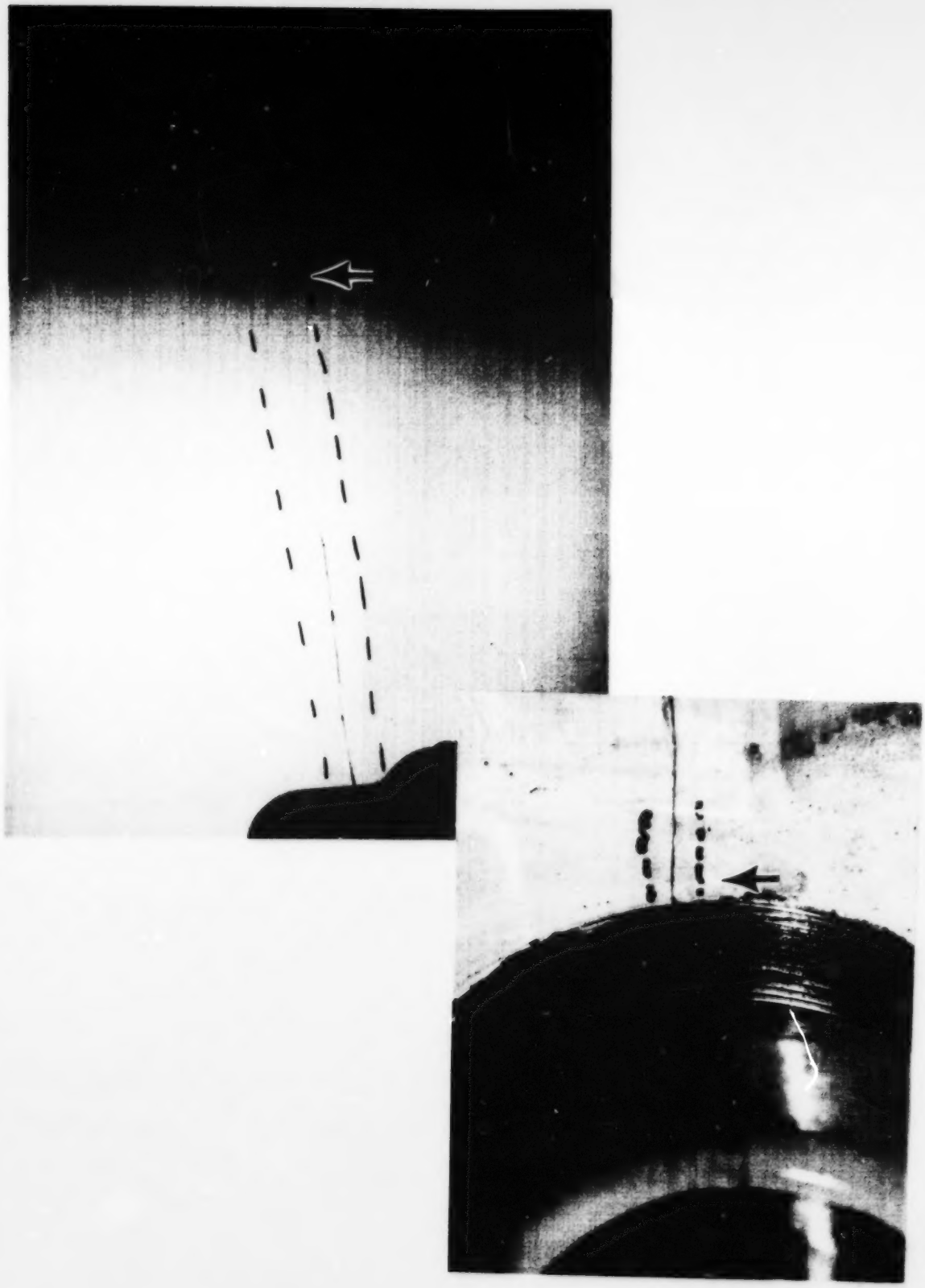

FIGURE 4 - DETAILS OF LARGE CRACK IN POLE 1 REGION

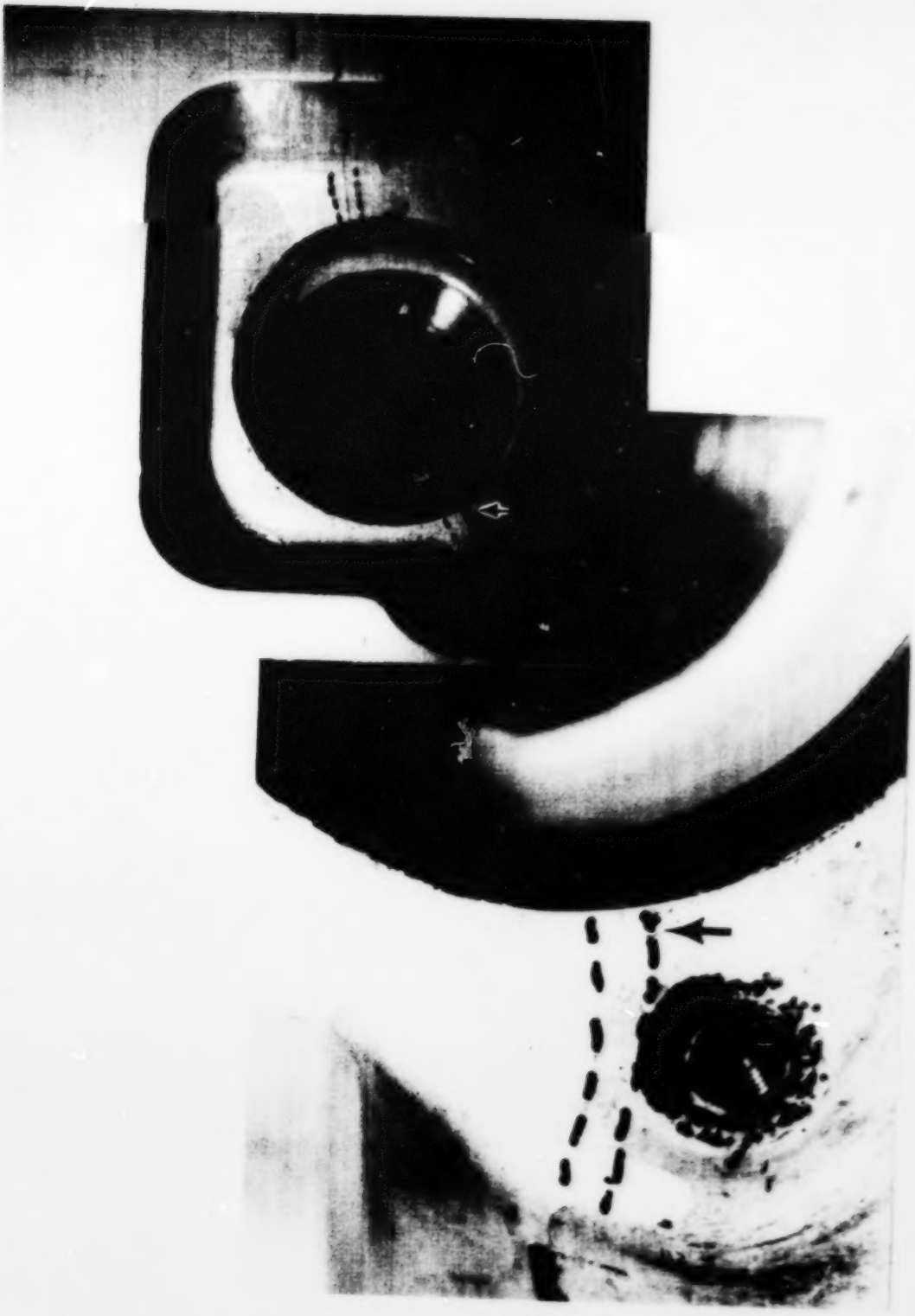

FIGURE 5 - DETAILS OF SMALL CRACK IN POLE 1 REGION

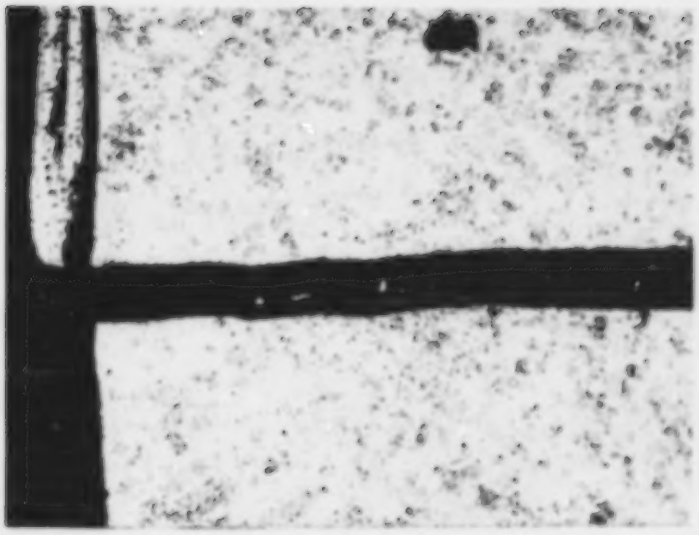

a) Metallographic replica from top edge of thread,large crack, X50

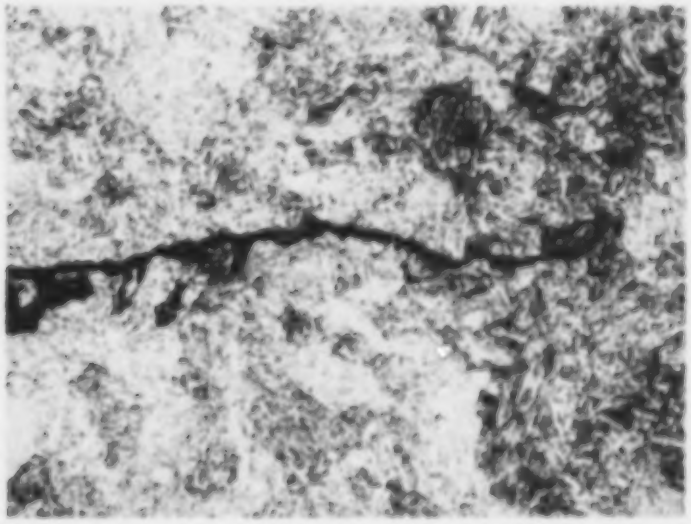

b)Metallographic replica from crack tip,large crack, X200

FIGURE 6 - DETAILS OF CRACKING FROM REPLICAS, POLE 1, UNIT 2

FIGURE 7 - RETAINING NUT, UNIT 4

FIGURE 8 - CROSS SECTION OF NUT, X1.3

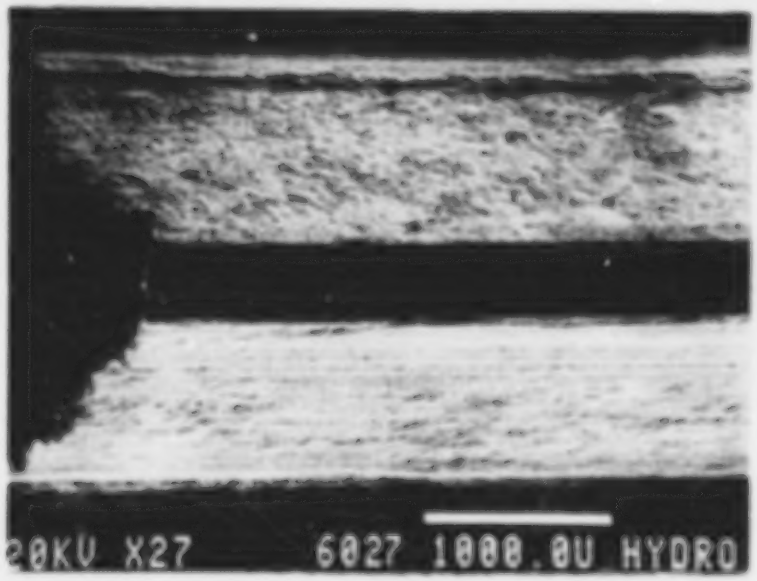

FIGURE 9 - DETAIL OF 4TH THREAD FROM TOP, showing fretting on the top surfaces.

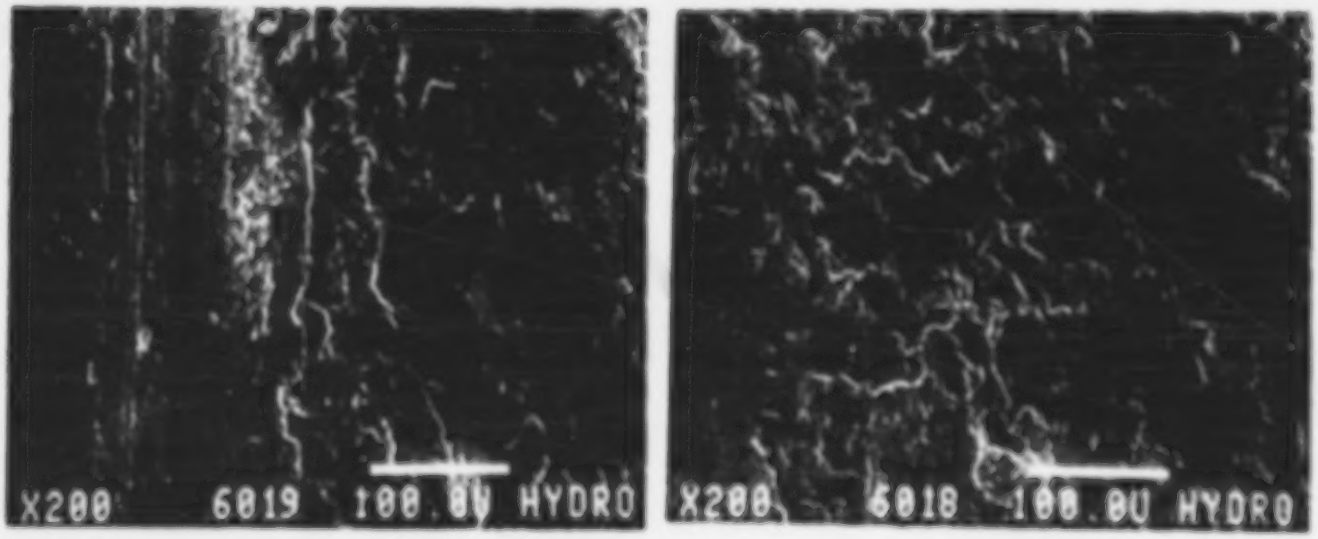

FIGURE 10 - SURFACE OF THREAD 3, showing typical fretted surface on the right and edge of fretted zone toward the root of the thread on left.

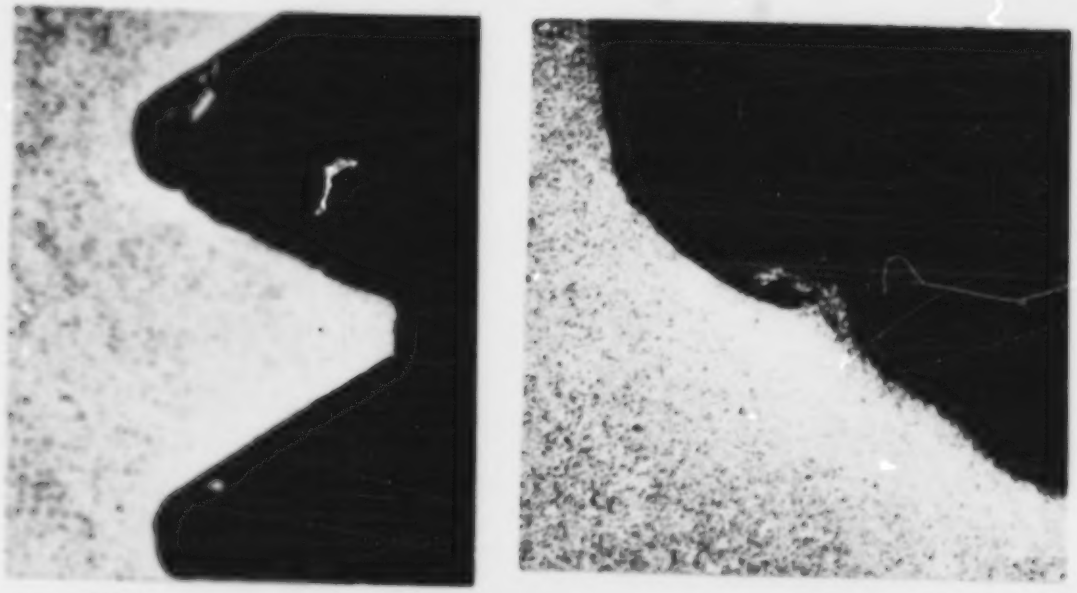

X20 X100

FIGURE 11 - CROSS SECTION OF THREAD 4, showing top surface fretting

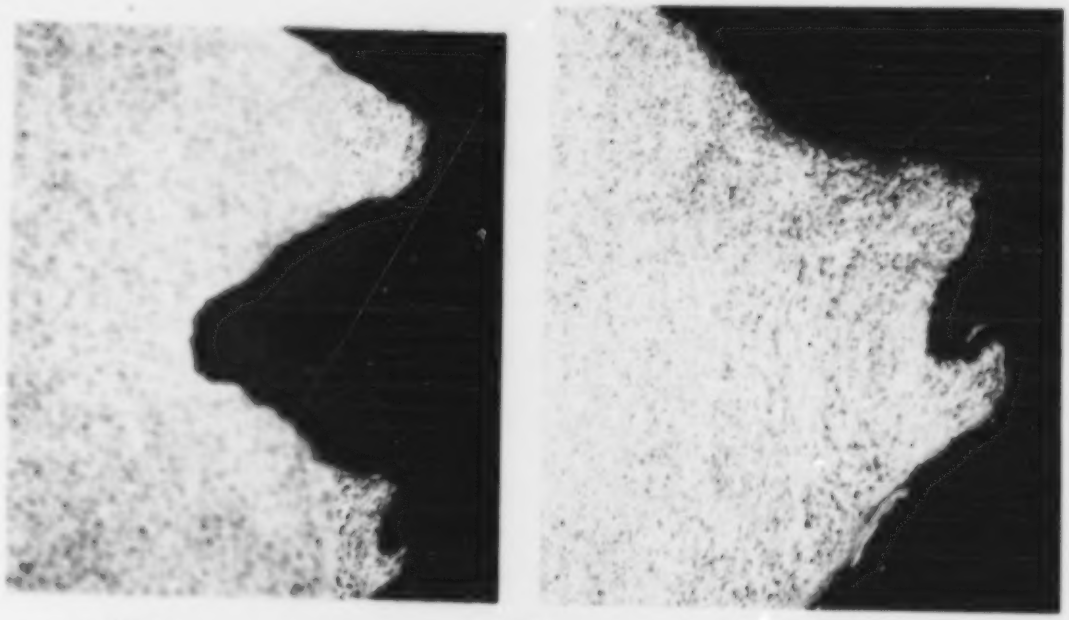

X20 X100

FIGURE 12 - CROSS SECTION OF THREAD 7, showing severe damage

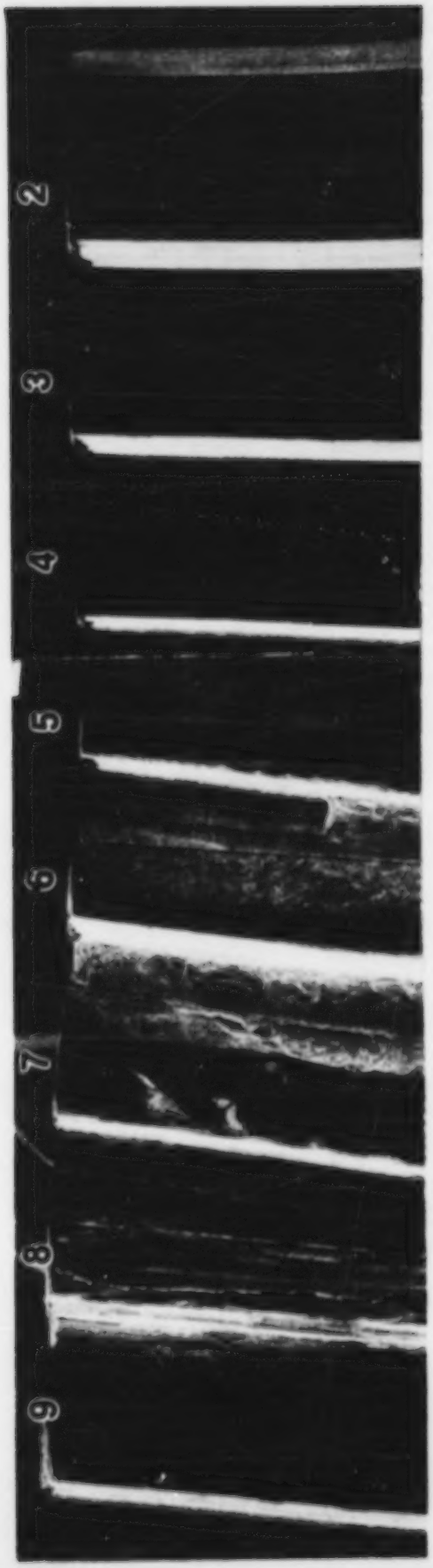

FIGURE 13 - VIEW OF THREAD SURFACES, tilted to reveal top surfaces, showing differences in damage from top to bottom, X11

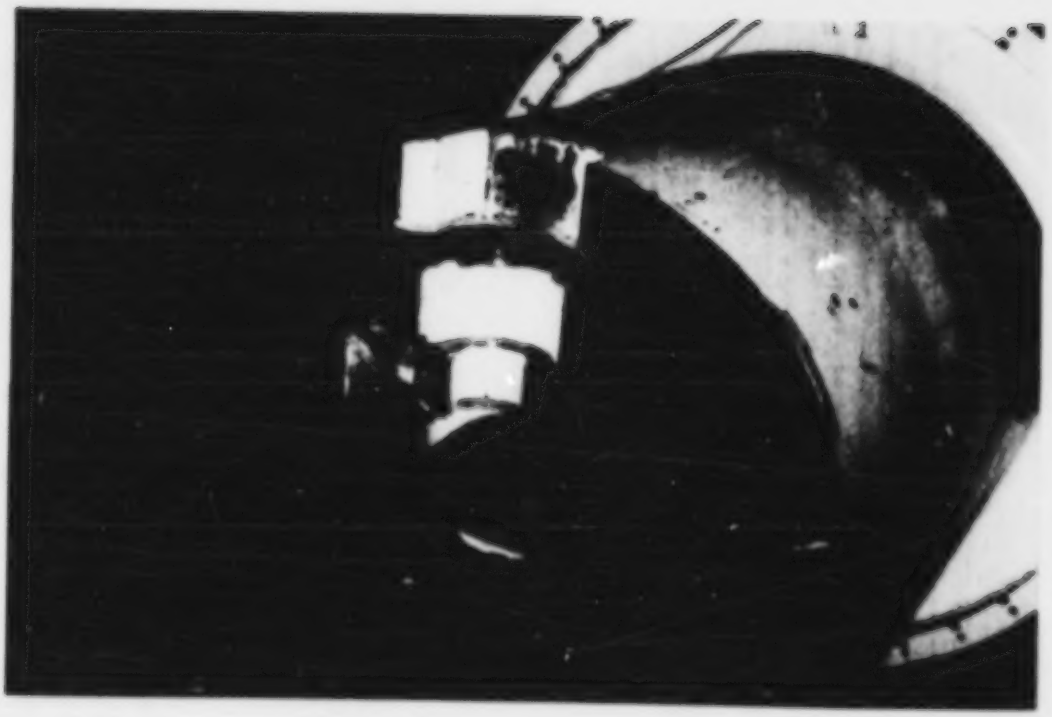

FIGURE 14 - GENERAL APPEARANCE OF SHAFT, immediately after breaking open

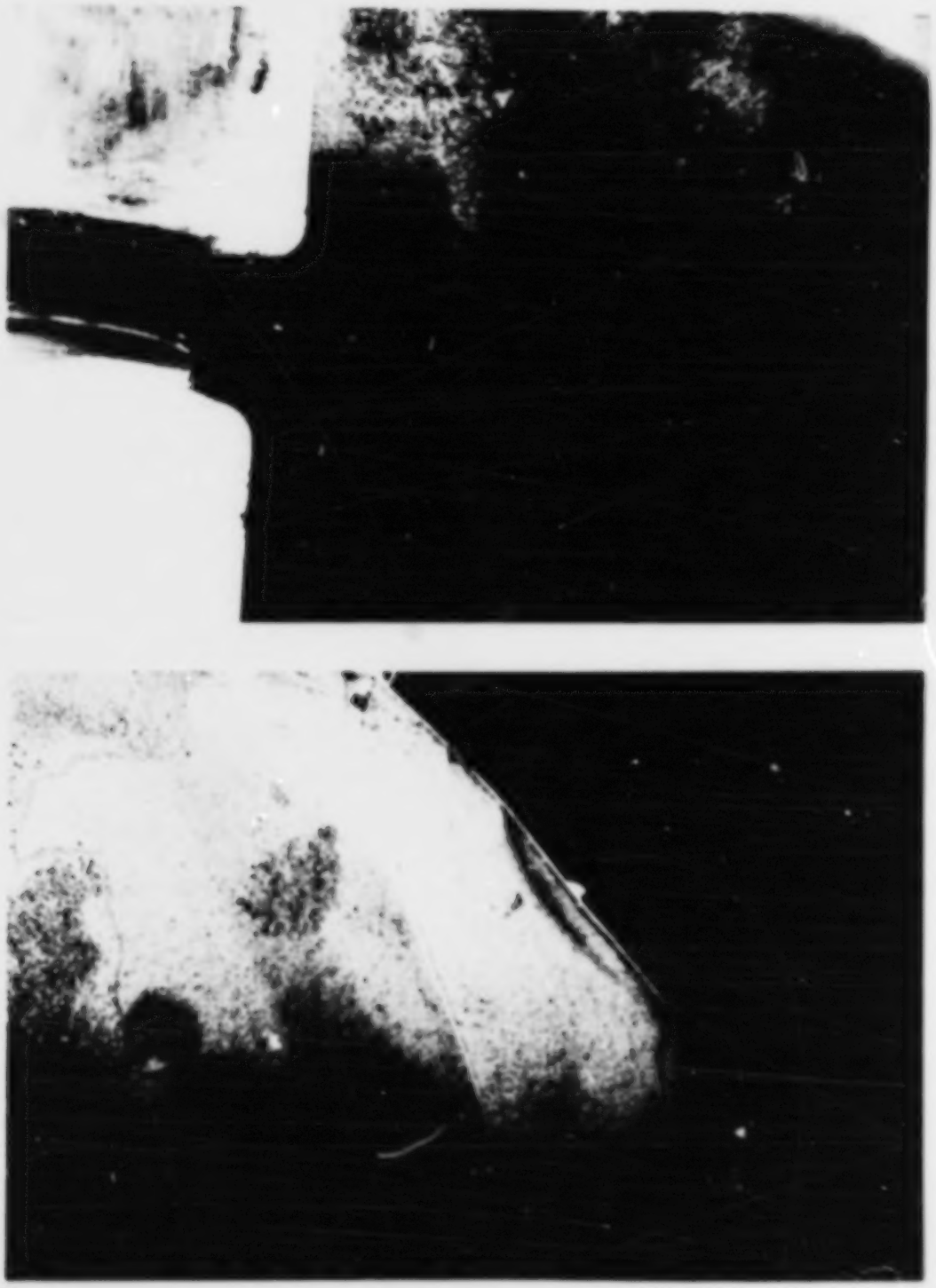

FIGURE 15 - DETAILS OF LARGE CRACK, thread region and crack extremity

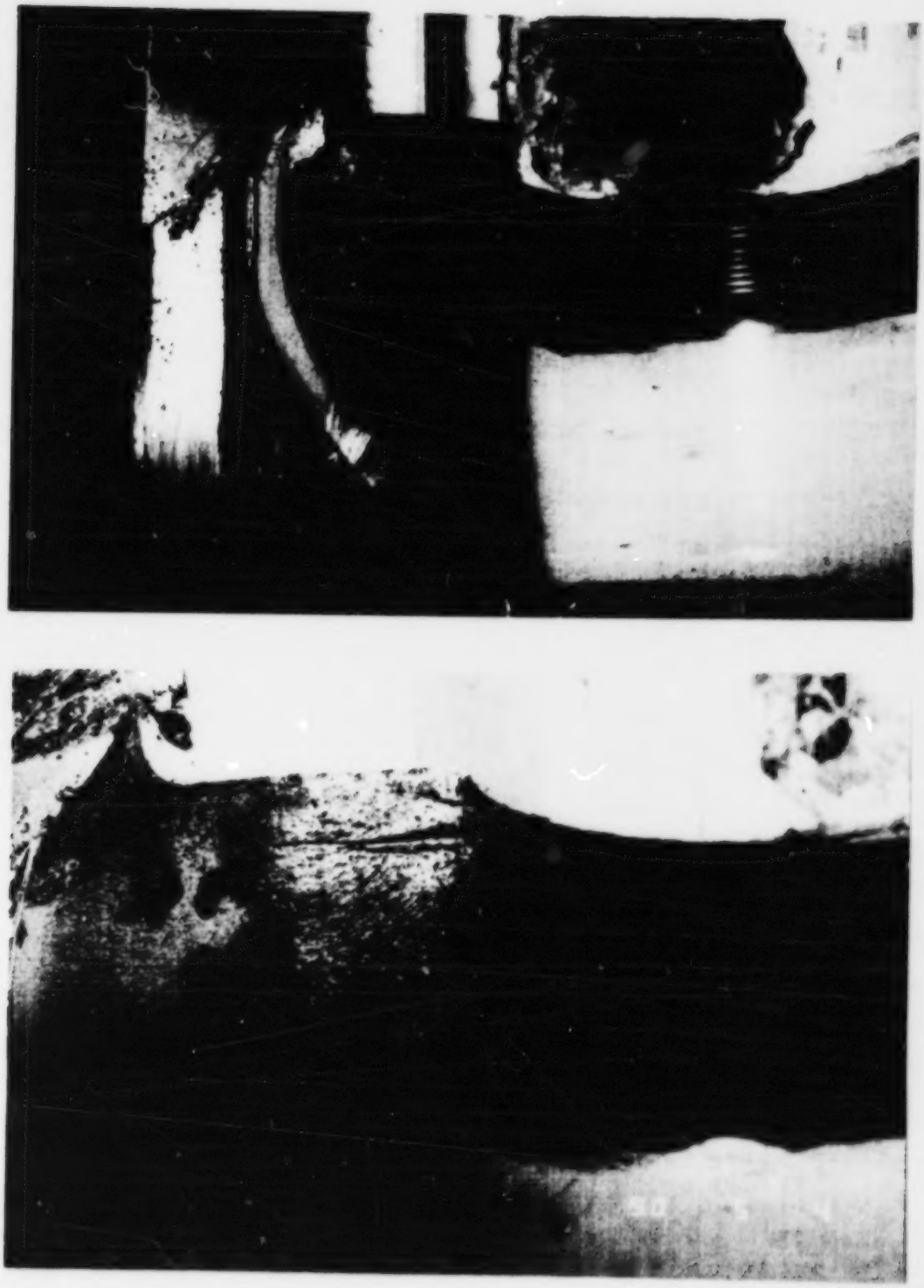

FIGURE 16 - DETAILS OF SMALL CRACK

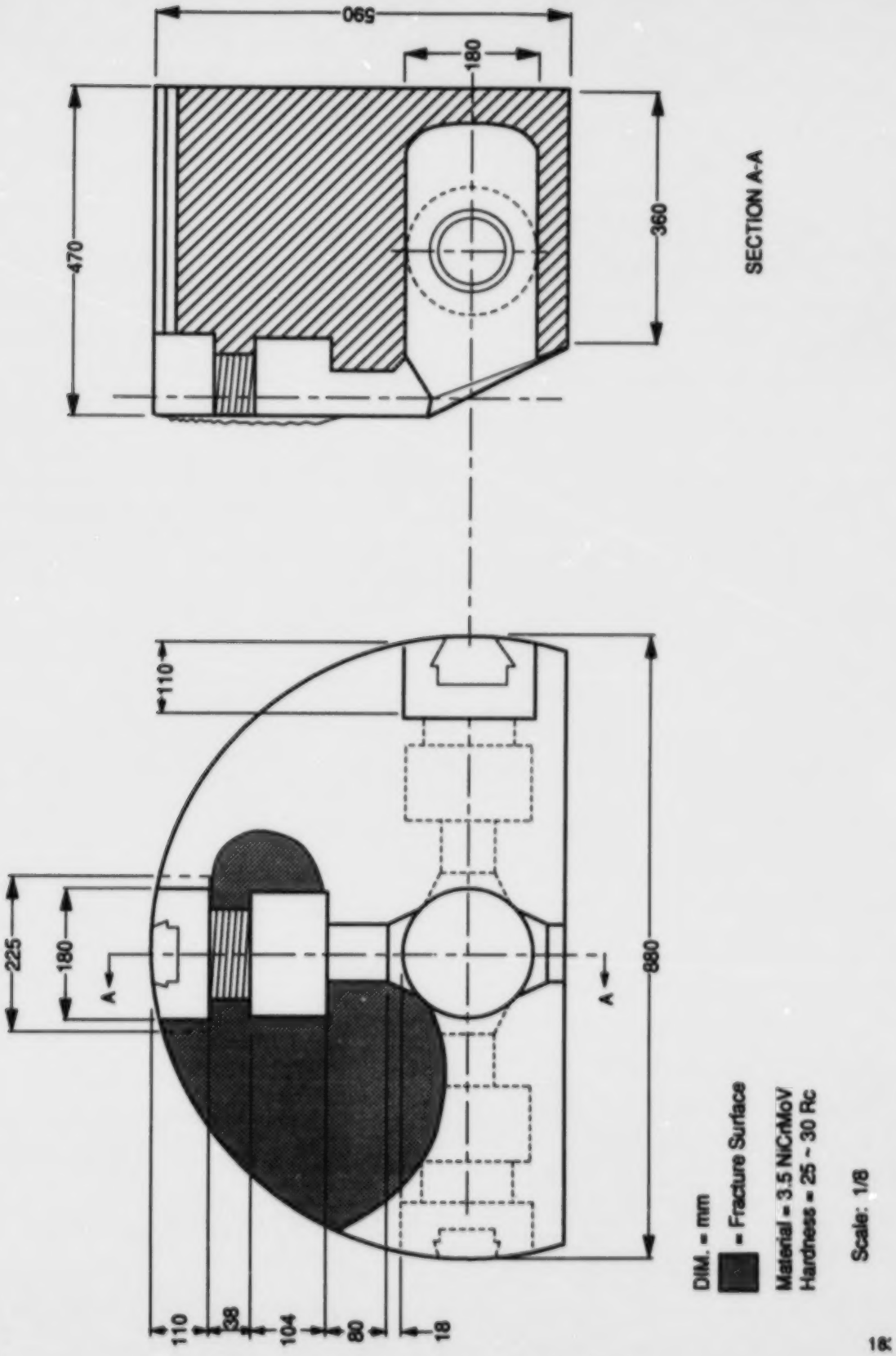

FIGURE 17 - SCHEMATIC OF SHAFT SECTION

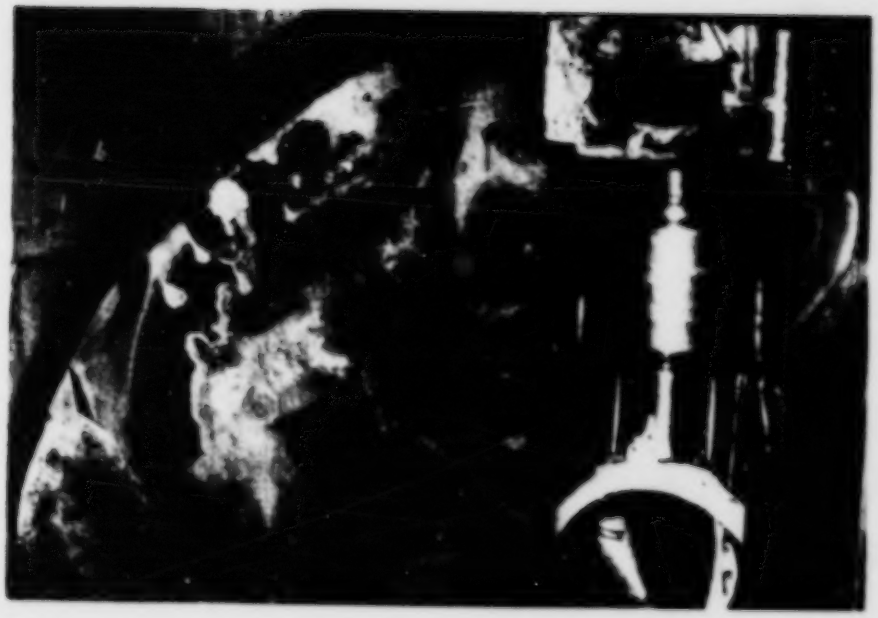

FIGURE 18 - GENERAL APPEARANCE OF CRACK SURFACES,after cleaning

FIGURE 19 - DETAILS OF LARGE CRACK, after cleaning

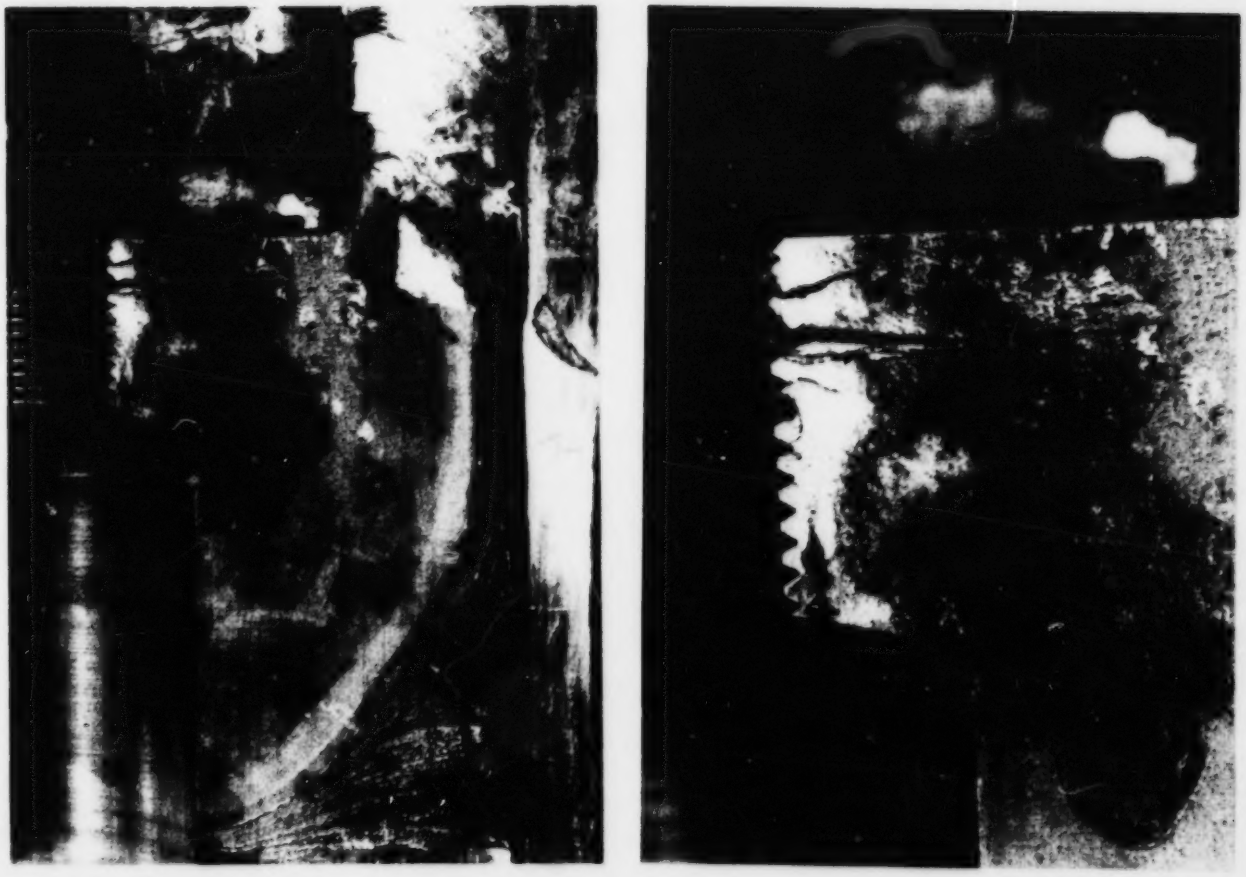

FIGURE 20 - DETAILS OF SMALL CRACK, after cleaning

RIM

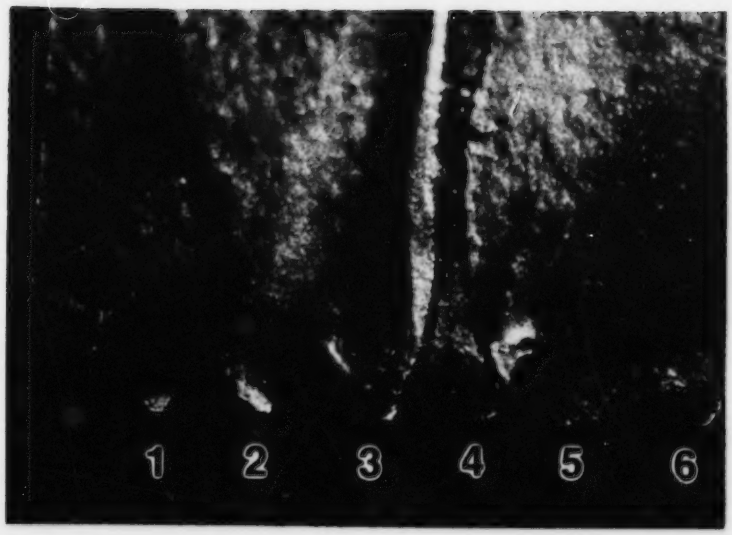

X5

FIGURE 21 - DETAILS OF INITIATION REGION AND THREAD NUMBERING

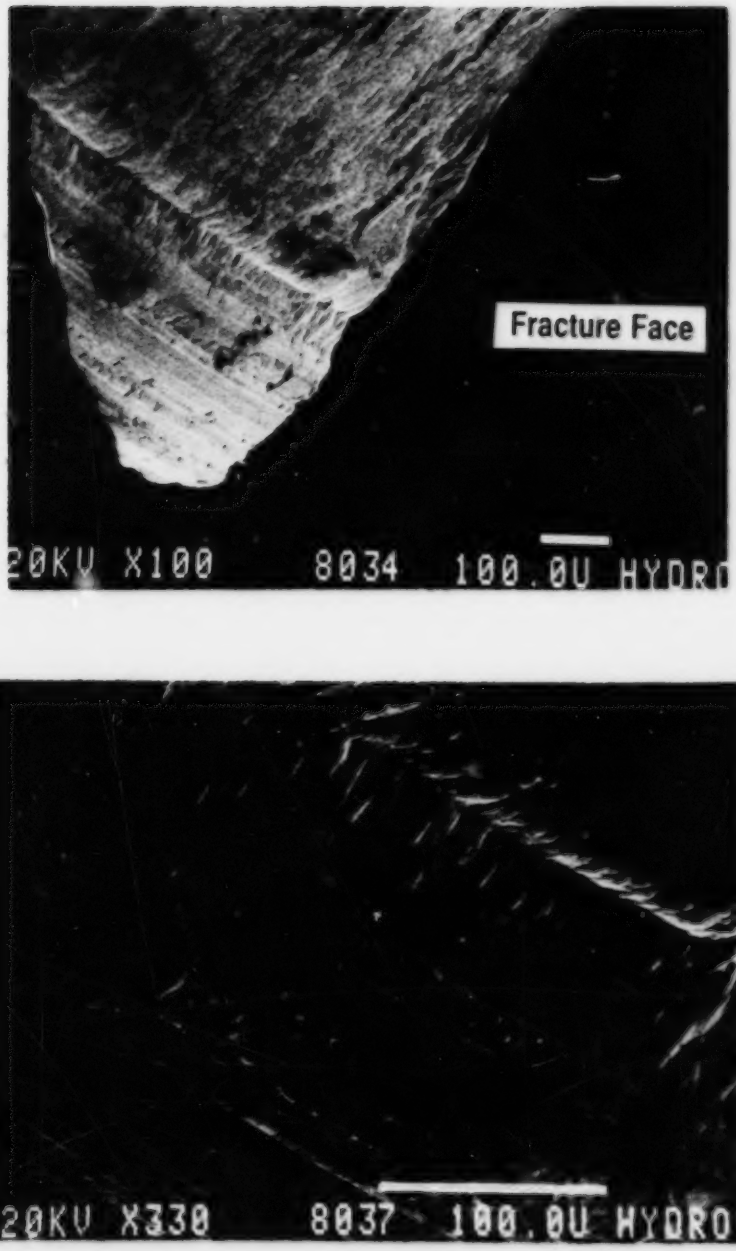

FIGURE 22 - FRETTING DAMAGE TO THREAD 1 ADJACENT TO FRACTURE, showing end of contact zone with nut surfaces and thread root surfaces

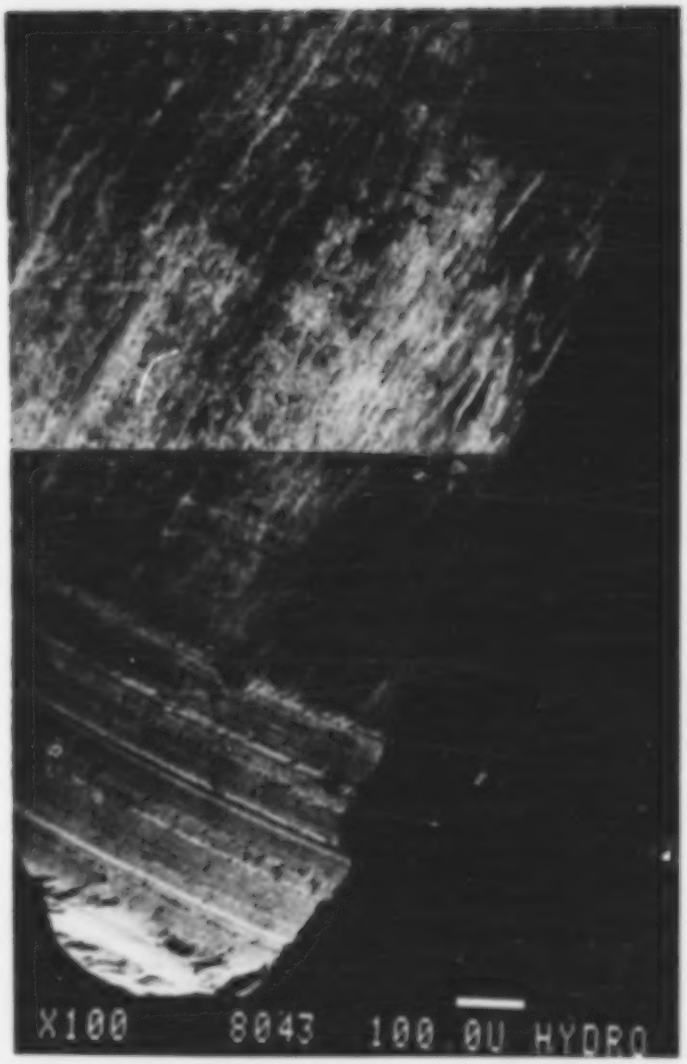

FIGURE 23 - LOWER FACE OF THREAD 2 ADJACENT TO FRACTURE, showing fretting damage

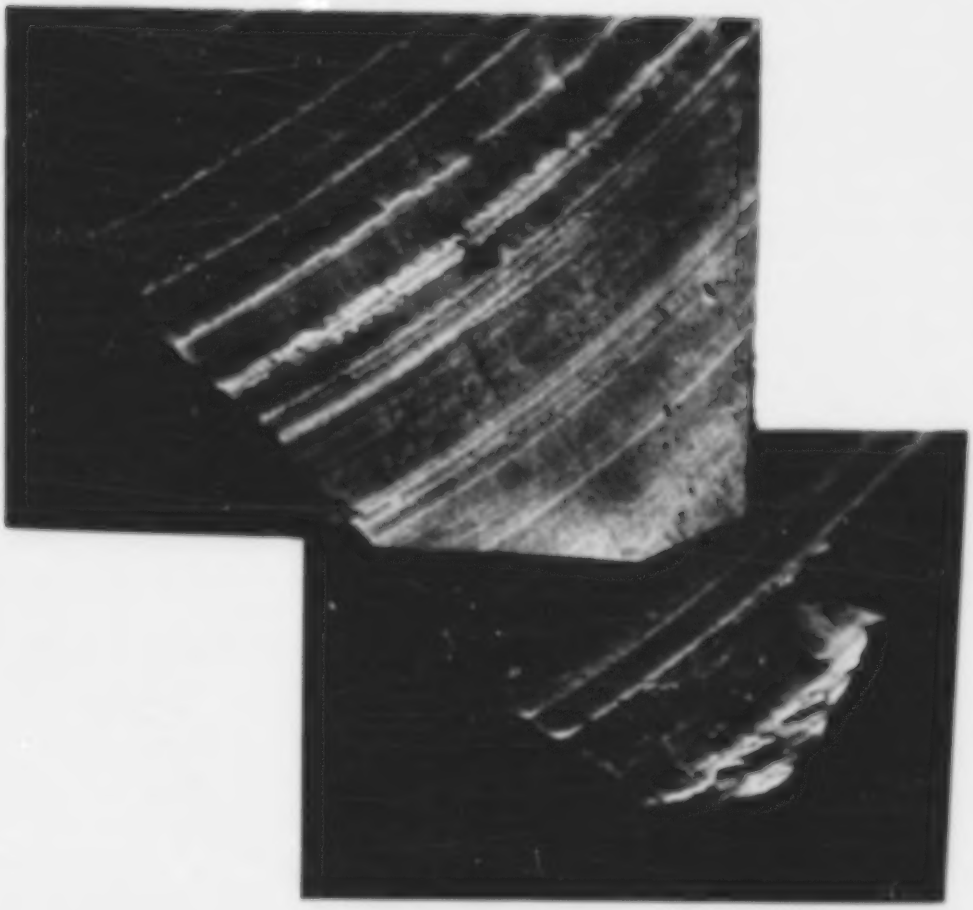

FIGURE 24 - UPPER FACE OF THREAD 2 ADJACENT TO FRACTURE, showing no damage, X100

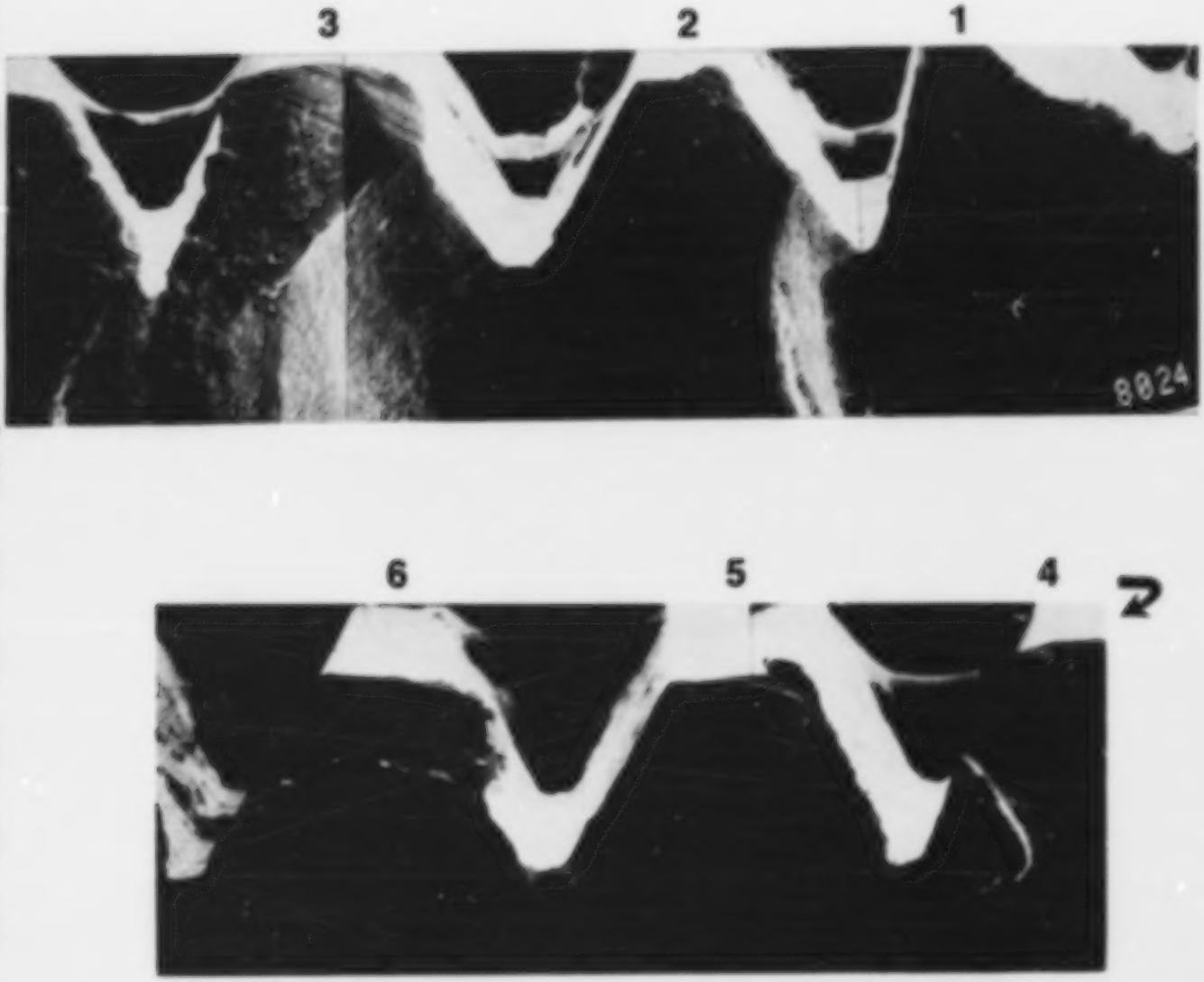

FIGURE 25 - FRACTURE SURFACE,SMALL CRACK, THREADS 1-6, showing general appearance of initiation zones, X20

a)x 30

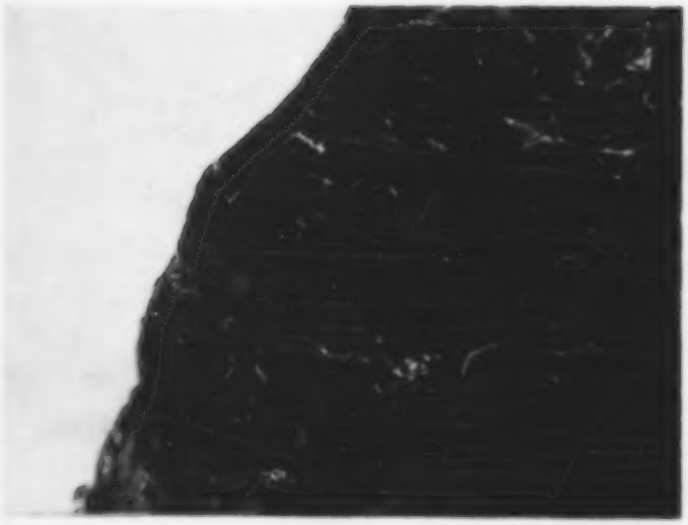

b) x300, possible initiation site

FIGURE 26 - FRACTURE SURFACE,SMALL CRACK,THREAD 1, showing possible initiation in thread flank area.

a)x 30

b) x50, possible initiation site

FIGURE 27 - FRACTURE SURFACE,SMALL CRACK,THREAD 2, showing possible initiation in thread flank area.

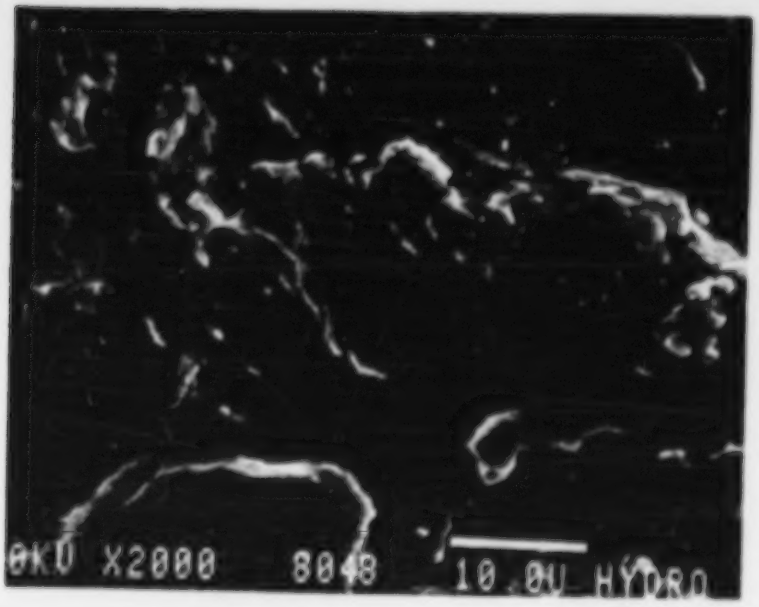

a) Early propagation, 1.5 cm from threads, X2000

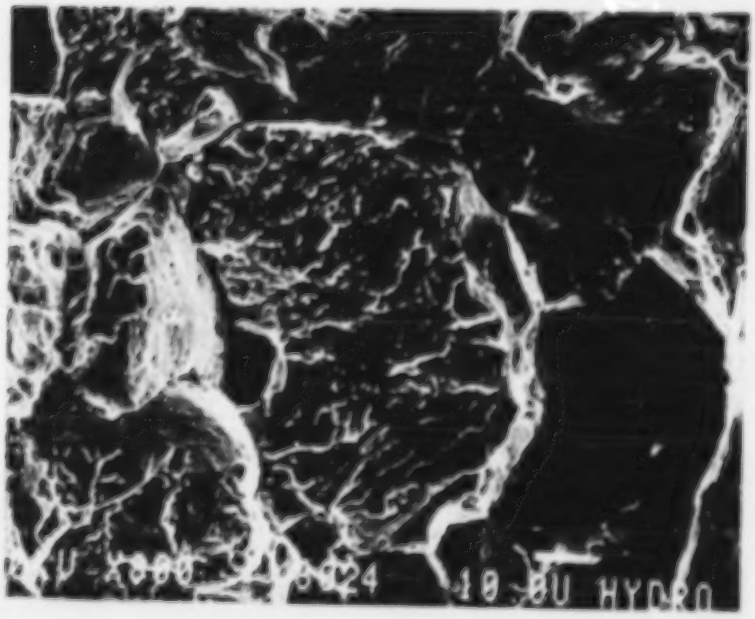

b) Late propagation, near tip of crack, X800

FIGURE 28 - FRACTURE SURFACE, SMALL CRACK,PROPAGATION ZONE FEATURES

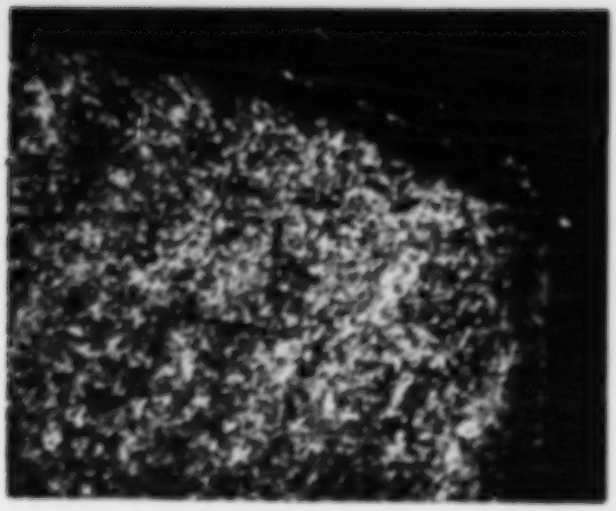

a) Section through thread root 4-5, X20

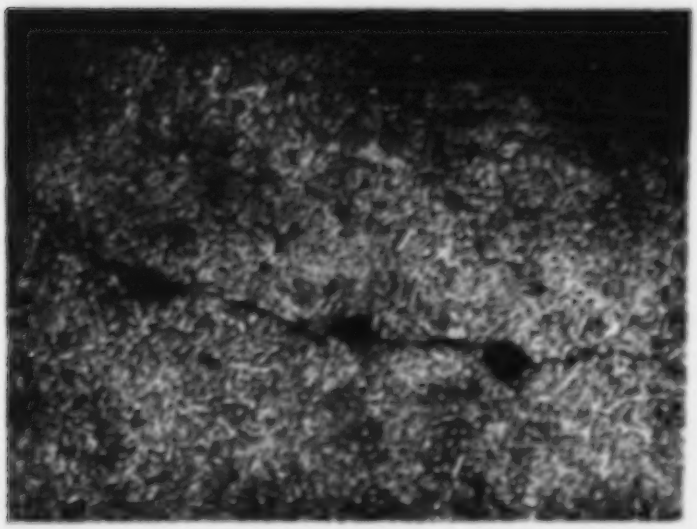

b) Portion of main and branch crack, X200

FIGURE 29 - METALLOGRAPHY OF SMALL CRACK

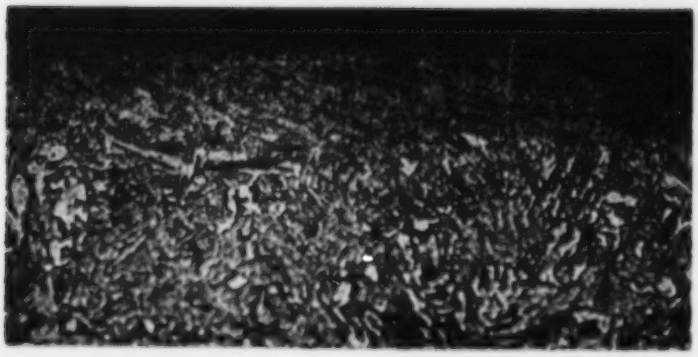

a) Main crack

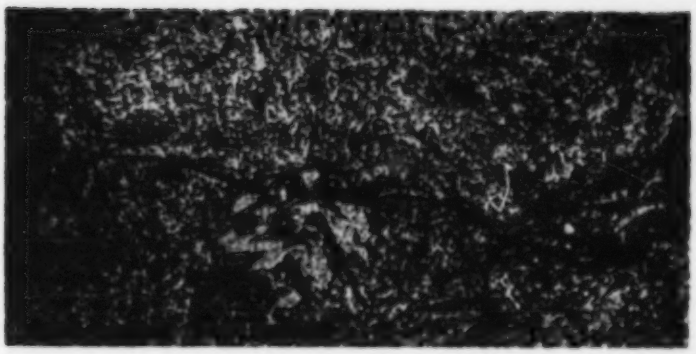

b) Branch from main crack

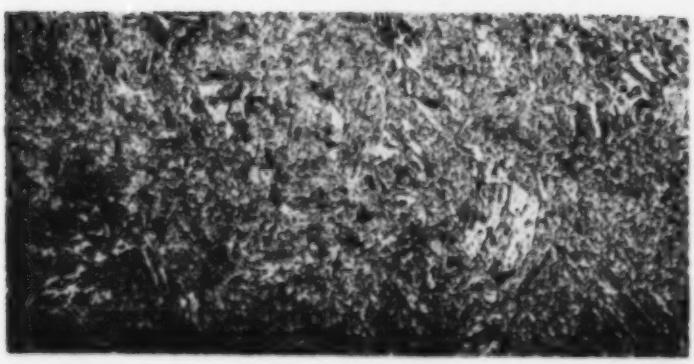

c) General microstructure

FIGURE 30 - MICROSTRUCTURE OF SMALL CRACK, showing partial intergranular crack path in branch, X500

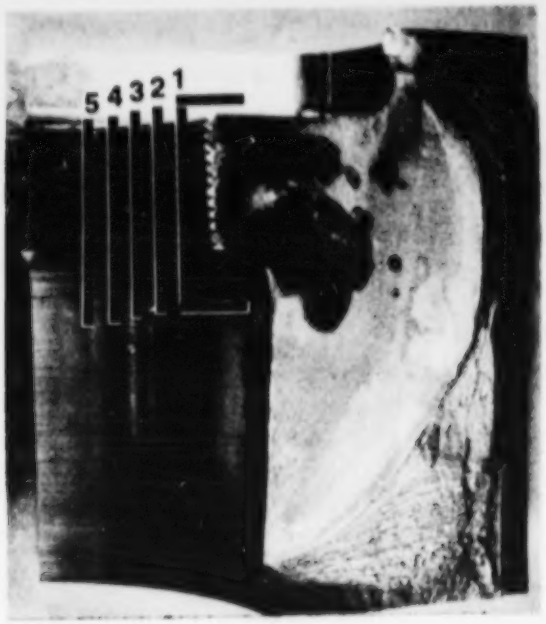

FIGURE 31 - LOCATION OF METALLOGRAPHIC SECTIONS, SMALL CRACK

FIGURE 32 - MICROSTRUCTURE OF THREAD ROOT #1, SMALL CRACK, X200

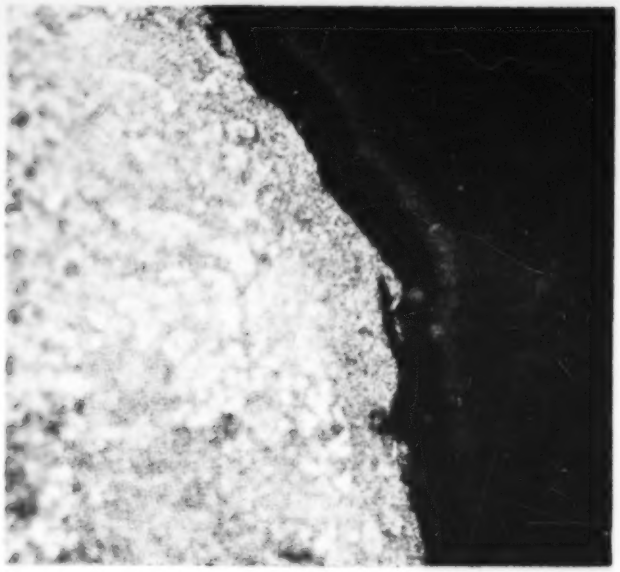

a) End of contact zone, X400

b) Typical damage, X200

FIGURE 33 - DETAILS OF FRETTING DAMAGE,THREAD FLANKS

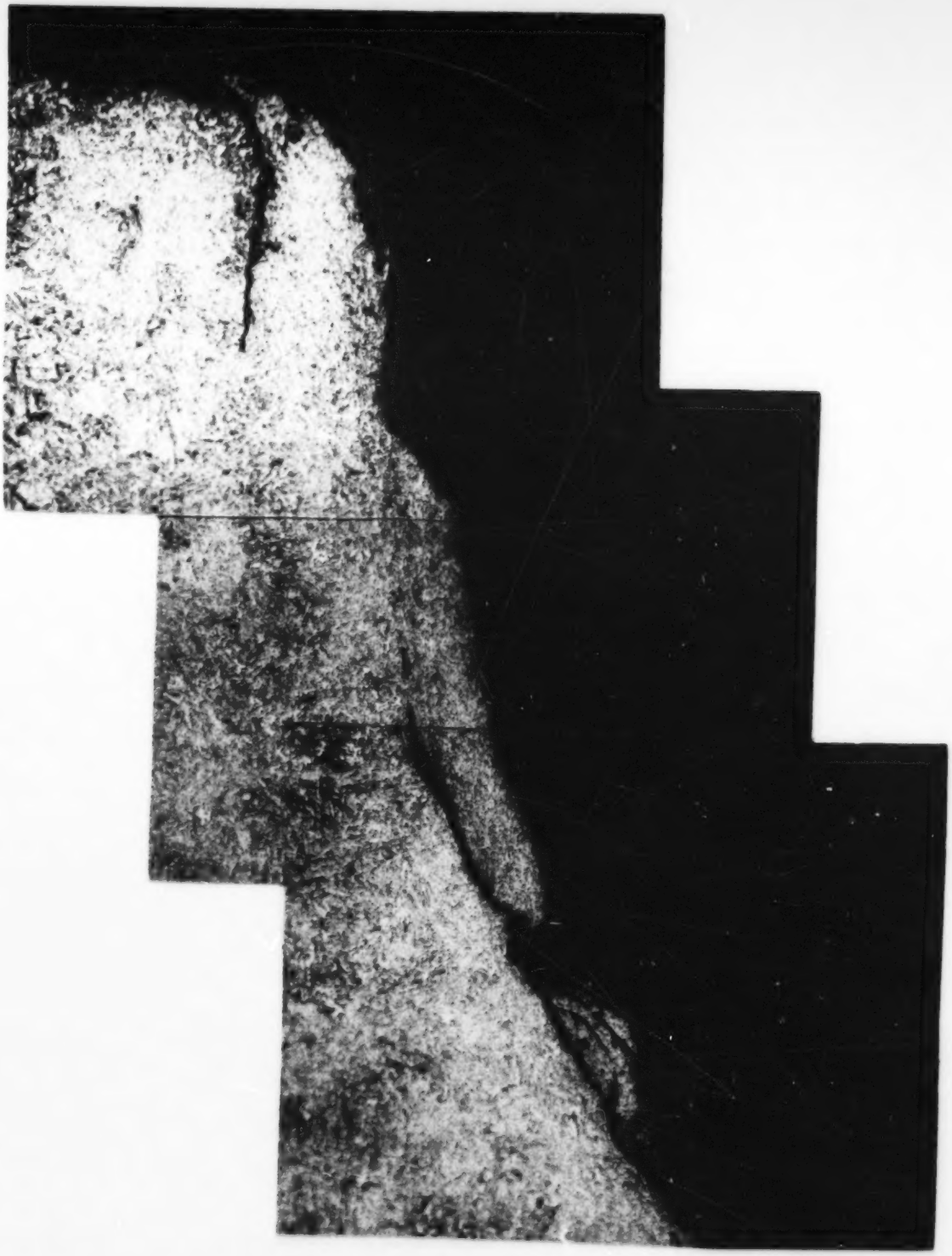

FIGURE 34 - MICROSTRUCTURE OF THREAD #6, SMALL CRACK, X200
showing severe fretting damage towards tip

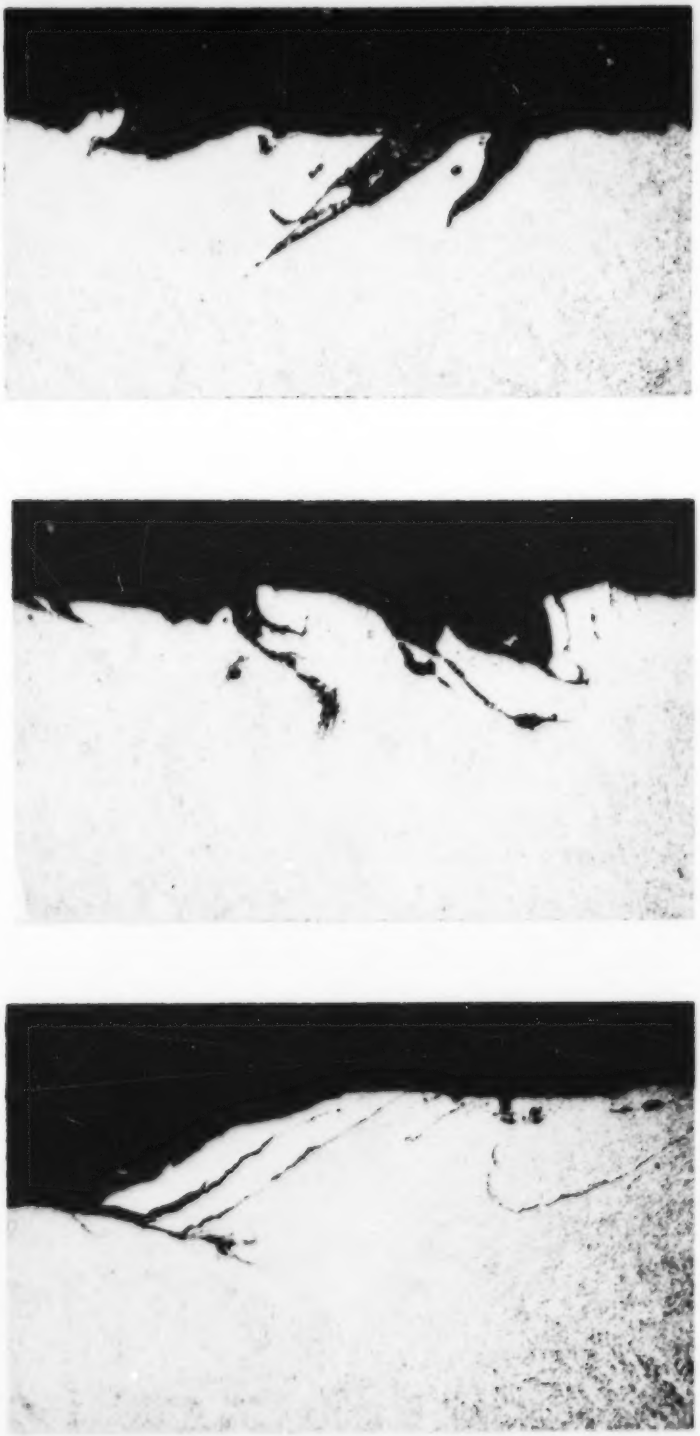

FIGURE 35 - TYPICAL FRETTING MICROCRACKS, X200

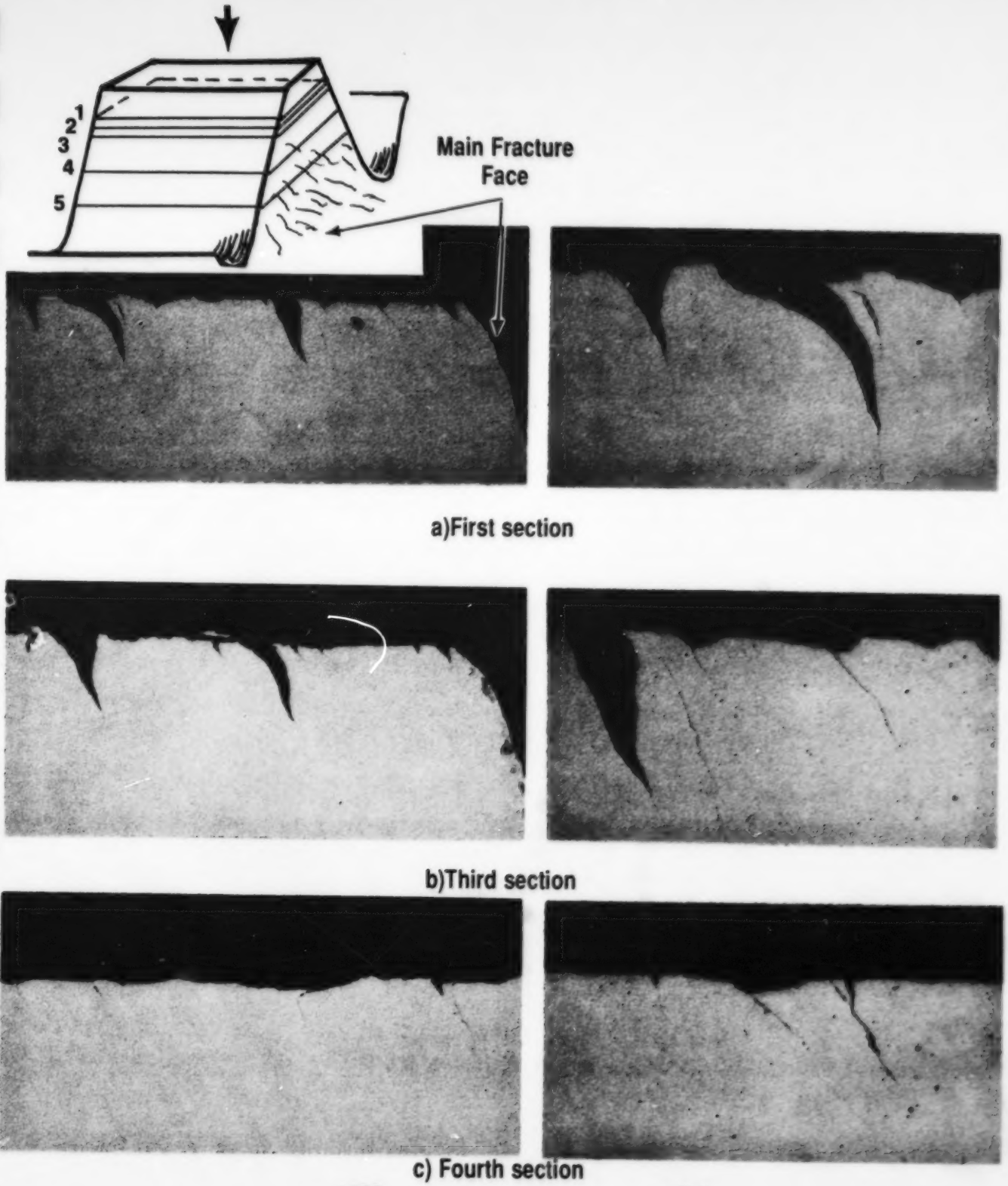

FIGURE 36 - FRETTING DAMAGE BEHIND SMALL CRACK

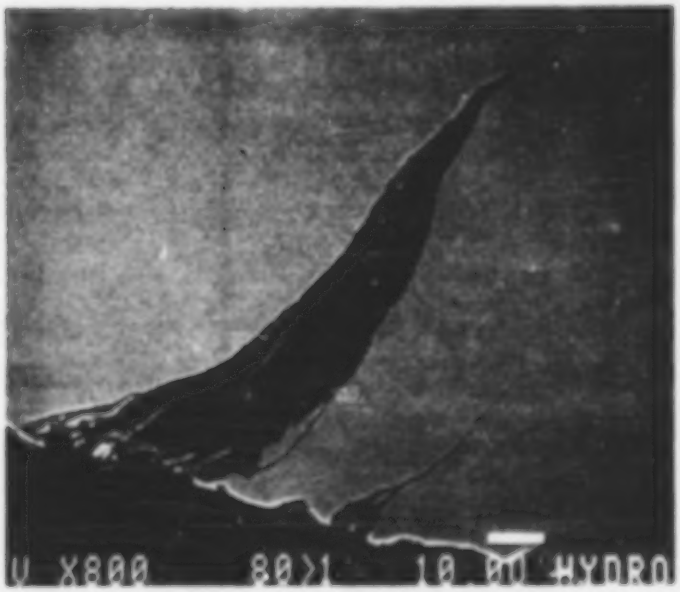

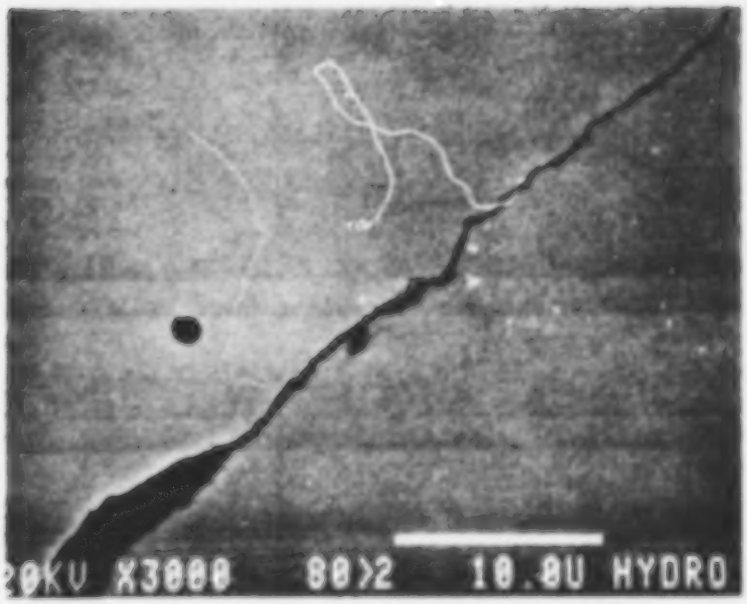

FIGURE 37 - DEVELOPMENT OF CRACKS FROM FRETTING DAMAGE, section 3

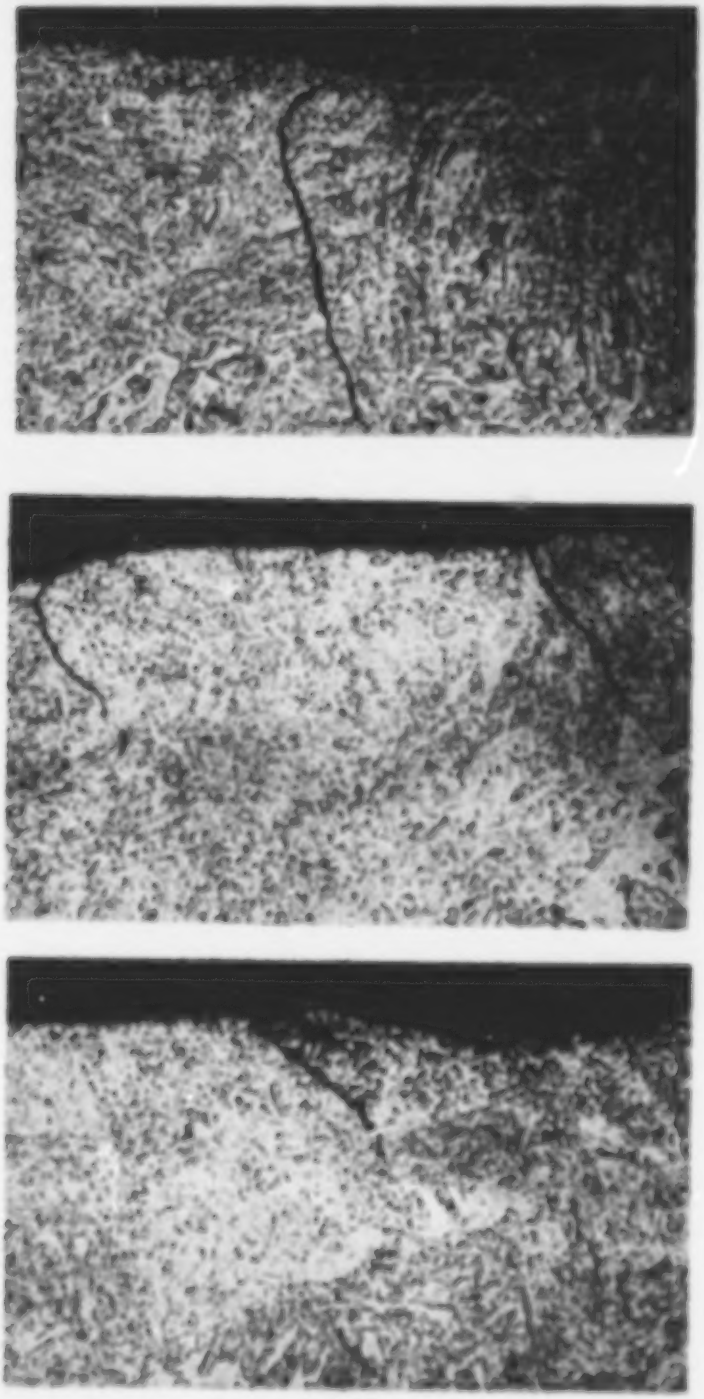

X1000

FIGURE 38 - FINE FRETTING CRACKS, section 5, main fracture face to right

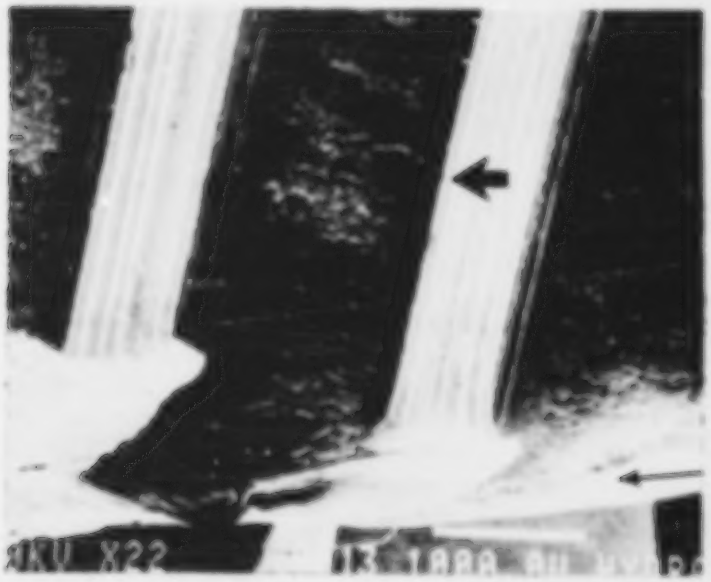

a) X22

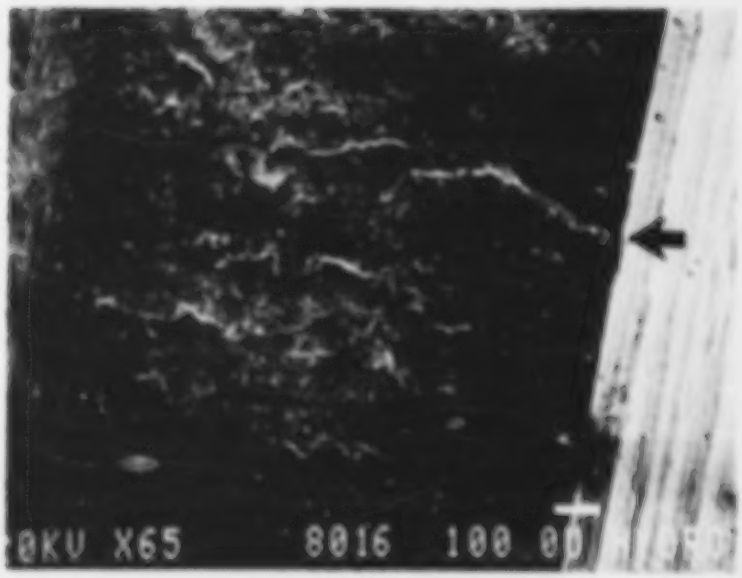

b) X65

FIGURE 39 - LOCATION OF SECONDARY CRACK BEHIND SMALL CRACK MAIN

a) x32

b) x500

FIGURE 40 - LOCATION AND MICROSTRUCTURE OF SECONDARY CRACK BEHIND SMALL CRACK

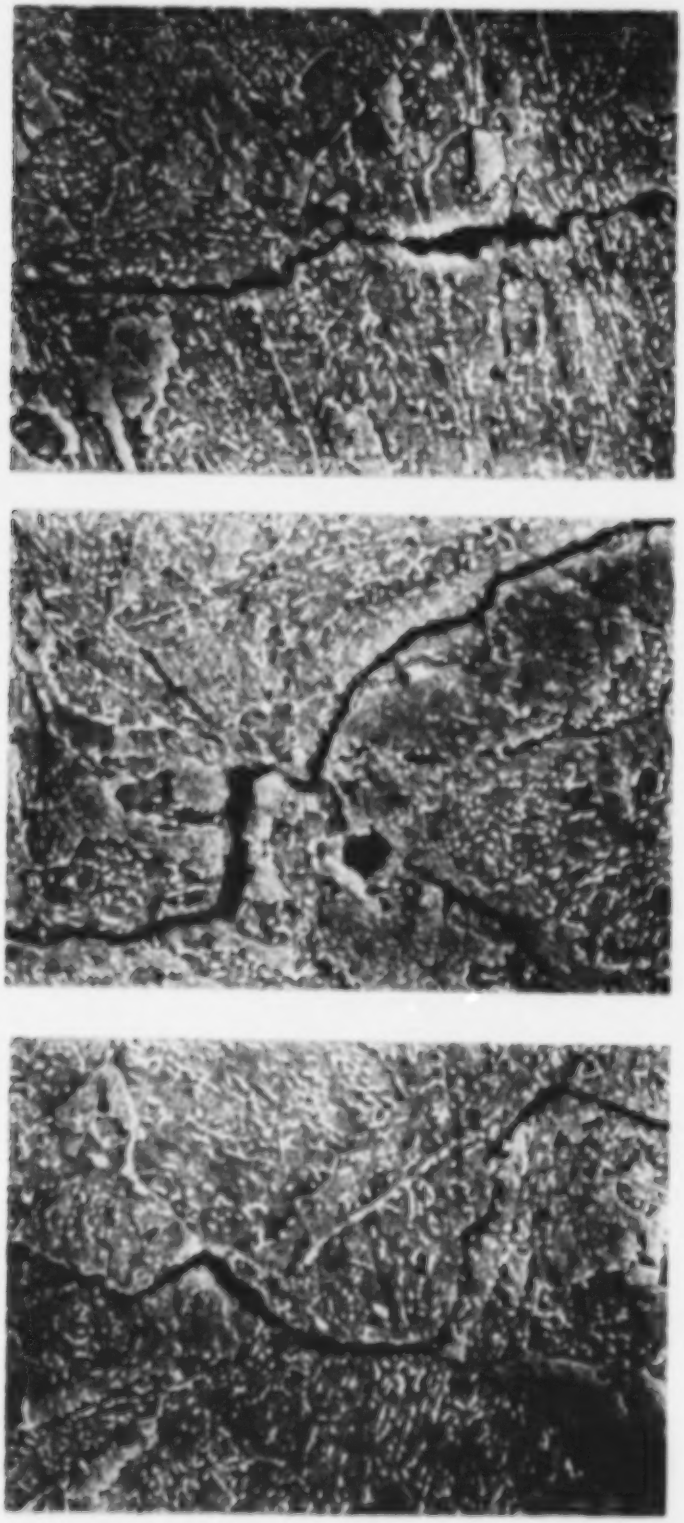

FIGURE 41 - DETAILS OF CRACK PATH OF SECONDARY CRACK, X4000

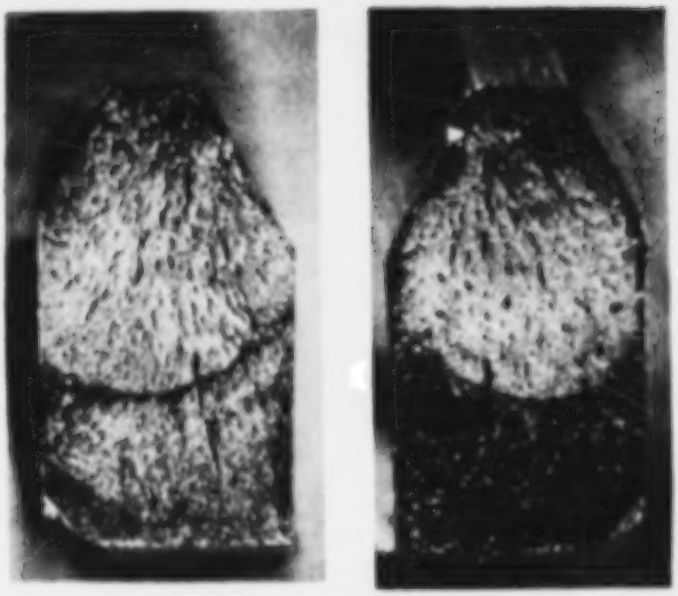

a) Matching fracture faces of secondary crack, x15

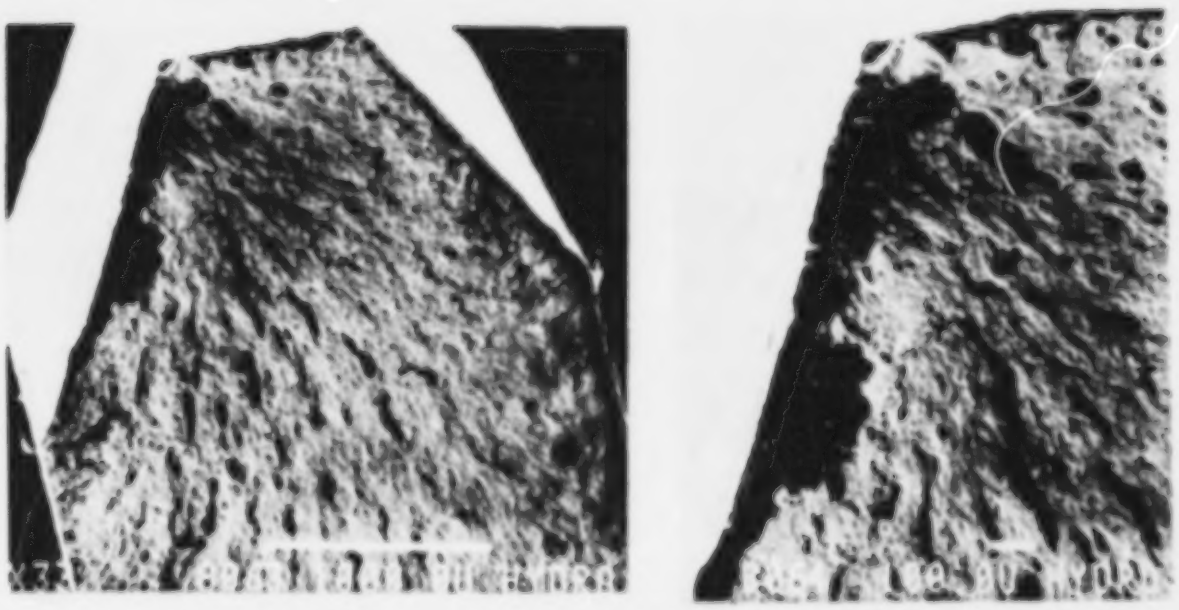

b) Initiation region, x33 and x 65

FIGURE 42 - FRACTOGRAPHY OF SECONDARY CRACK

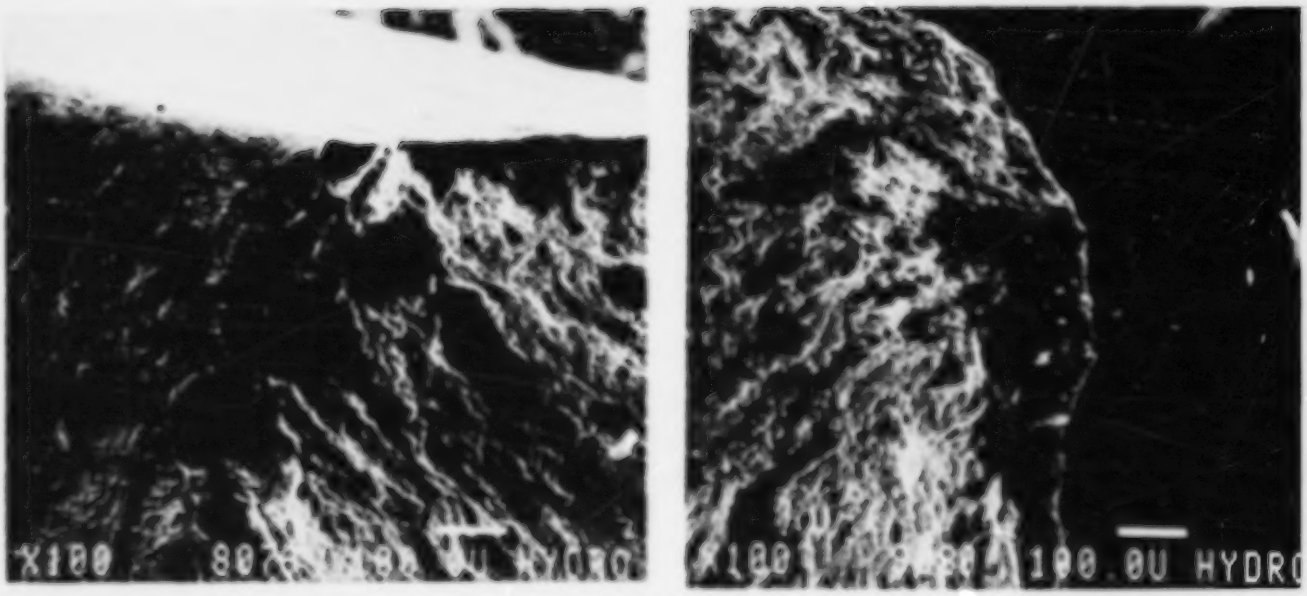

FIGURE 43 - INITIATION REGION OF SECONDARY CRACK, matching halves, x100

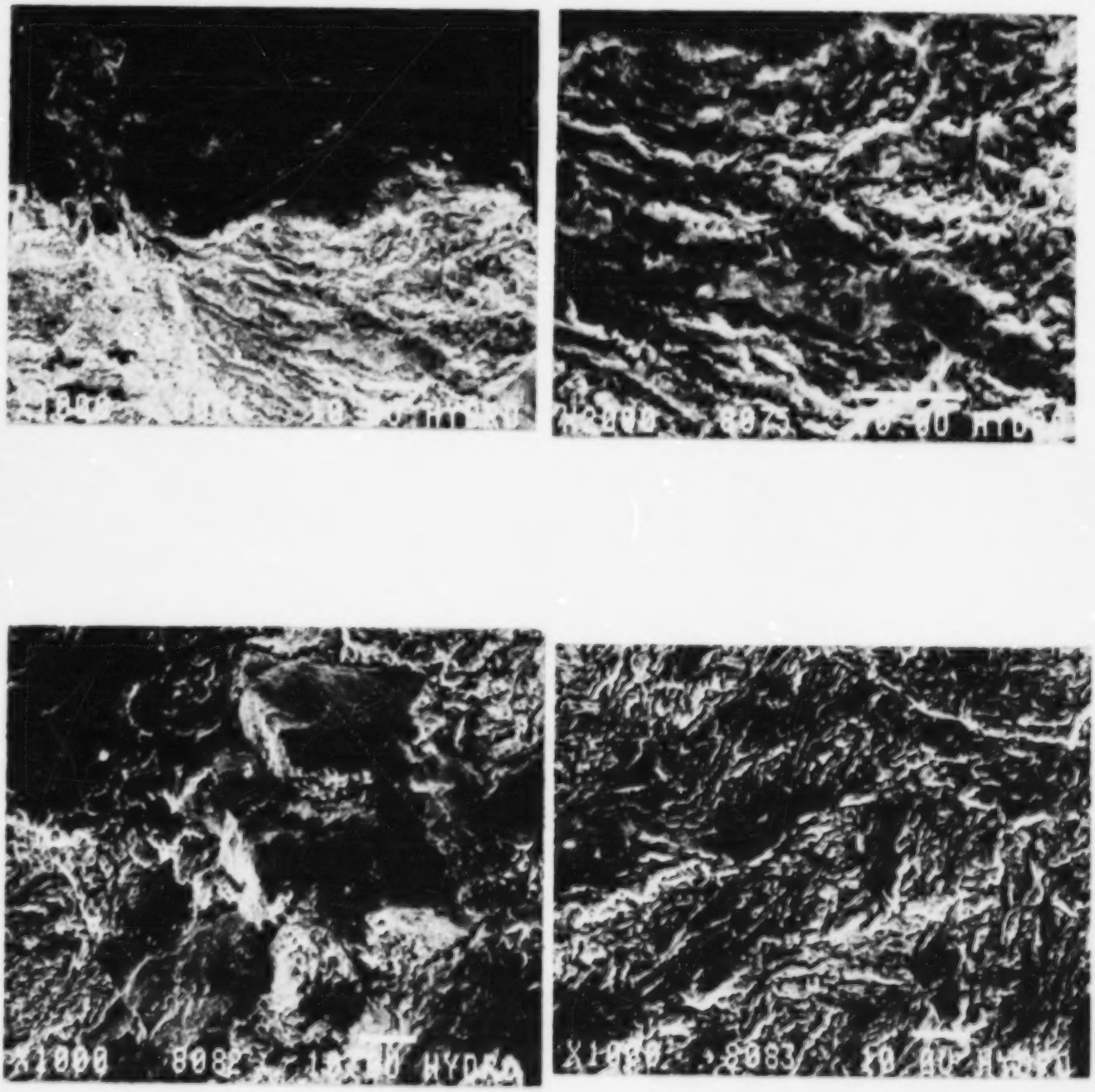

b) Propagation region, x1000

FIGURE 44 - FRACTOGRAPHIC DETAILS OF SECONDARY CRACK

a) x35

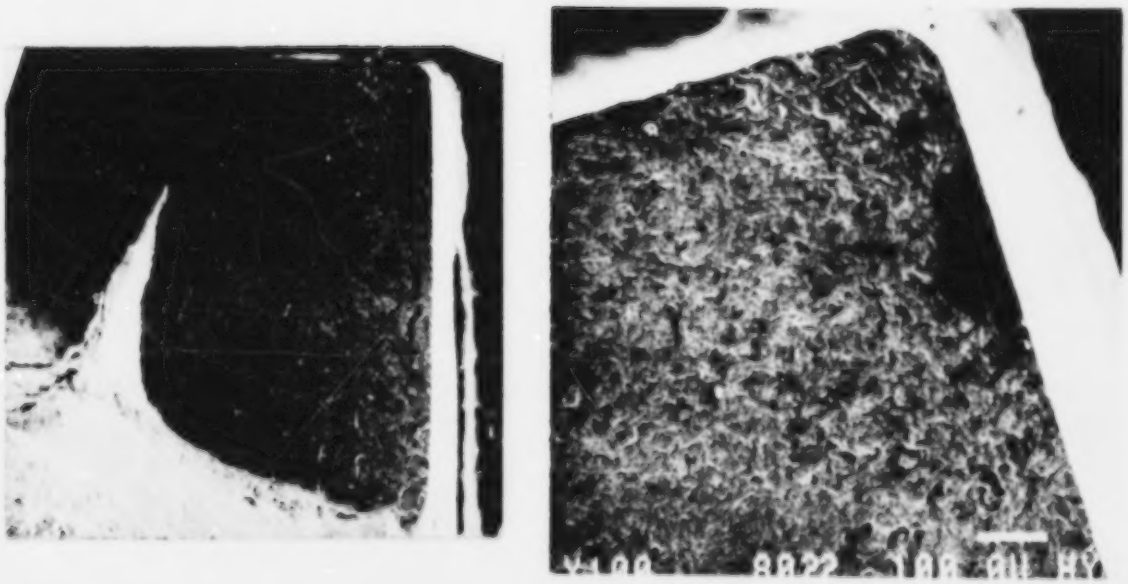

a) x33 and x100

FIGURE 45 - FRACTOGRAPHY OF SECONDARY CRACK, ABB half of fracture

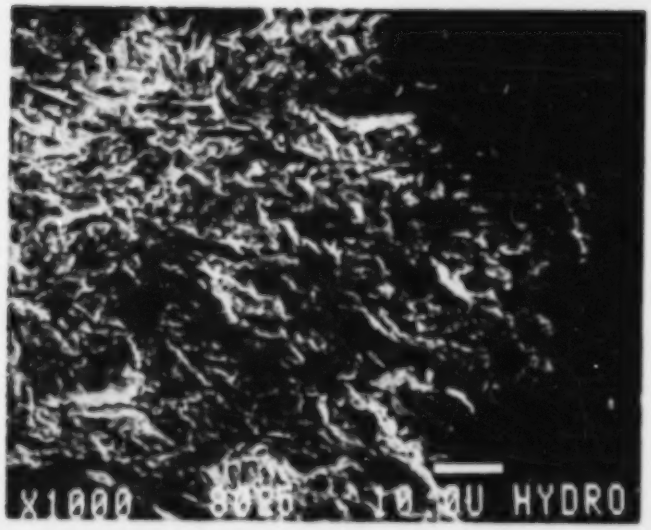

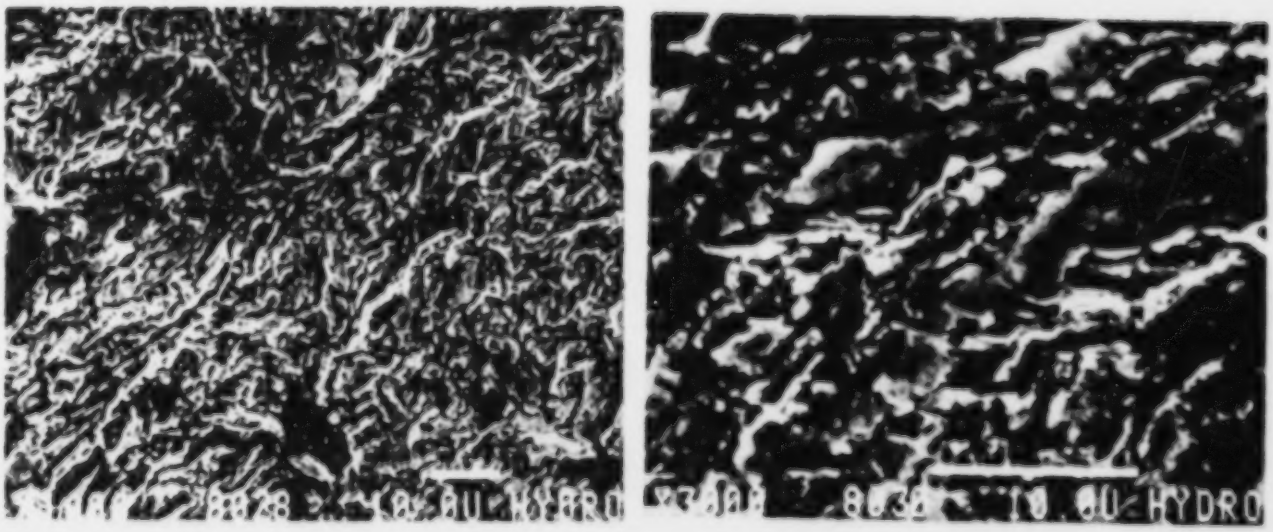

FIGURE 46 - DETAILED FRACTOGRAPHY, secondary crack, ABB half, X1000, X3000

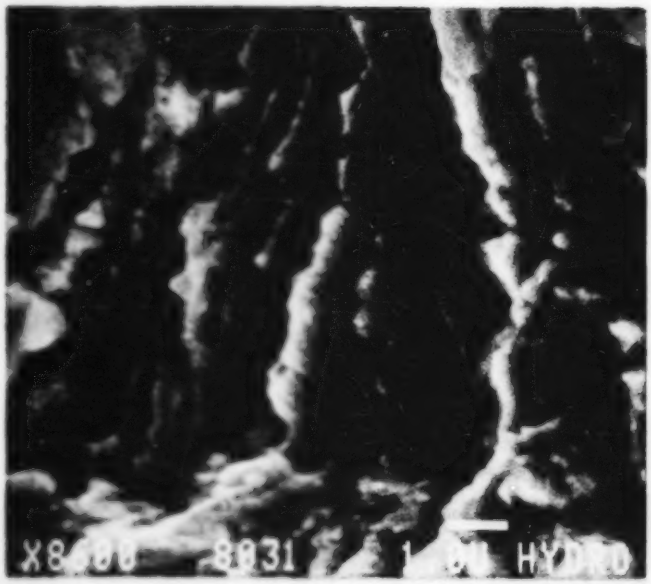

b) TEM fractograph x20000

FIGURE 47 - DETAILED FRACTOGRAPHY,secondary crack, ABB half

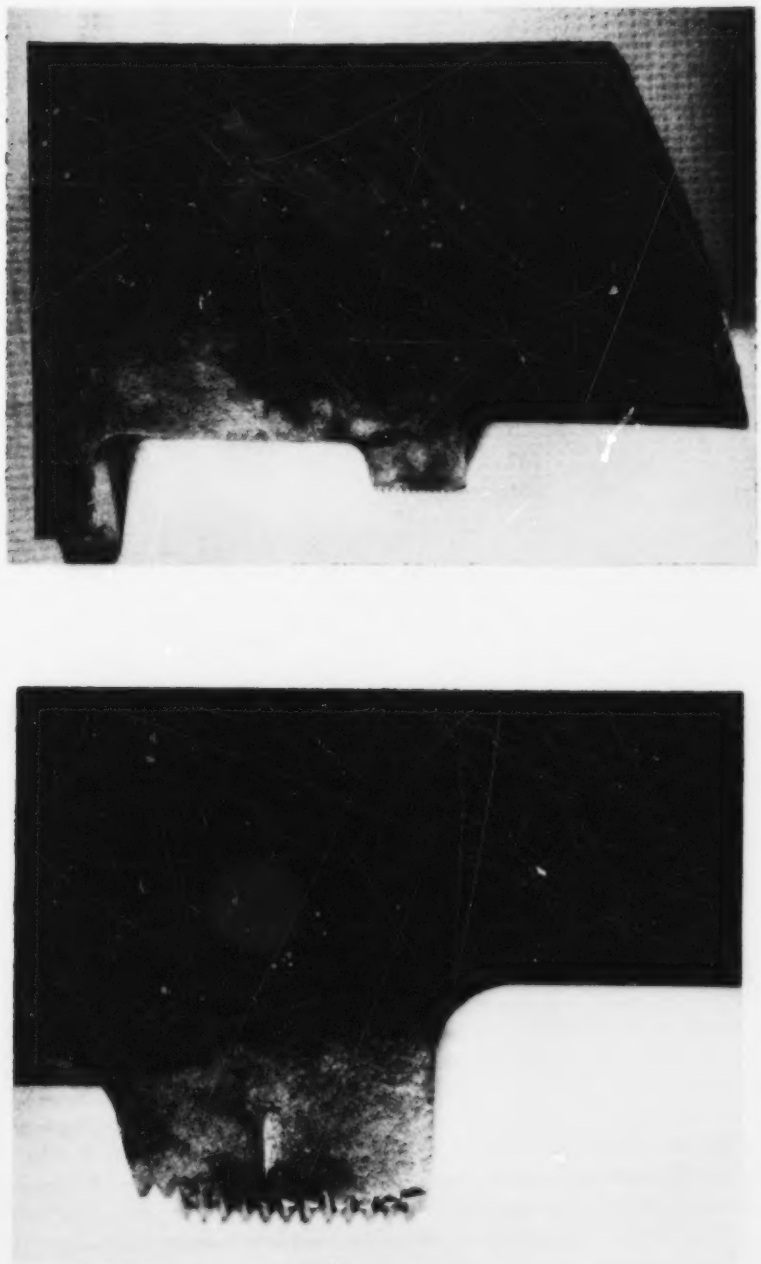

FIGURE 48 - GENERAL APPEARANCE OF INITIATION ZONE OF LARGE CRACK

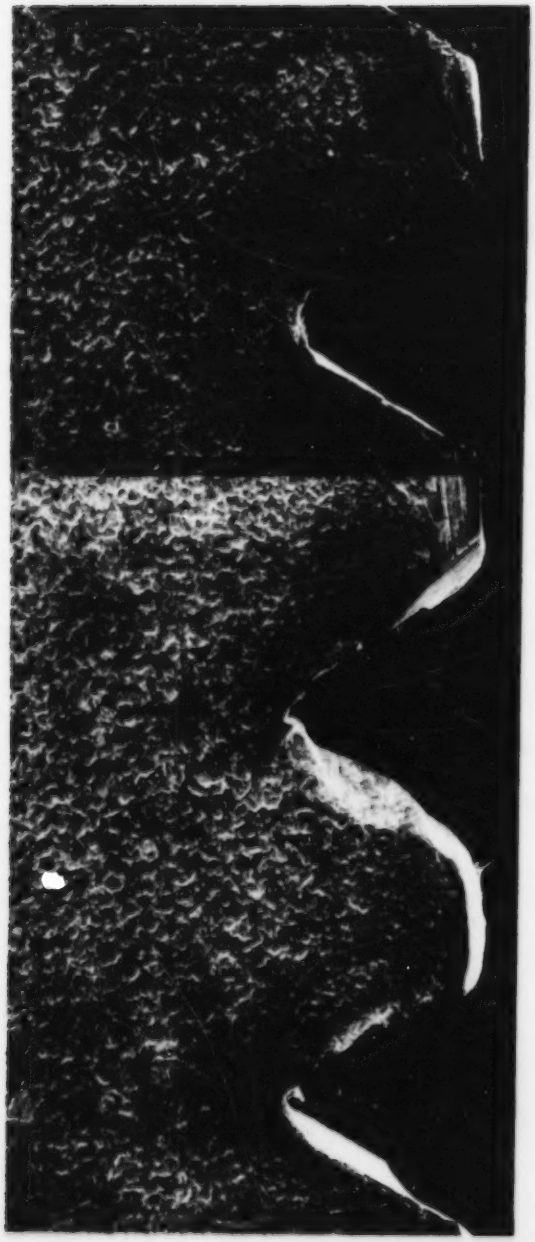

FIGURE 49 - FRACTURE SURFACES, THREADS 1-3, LARGE CRACK, X20

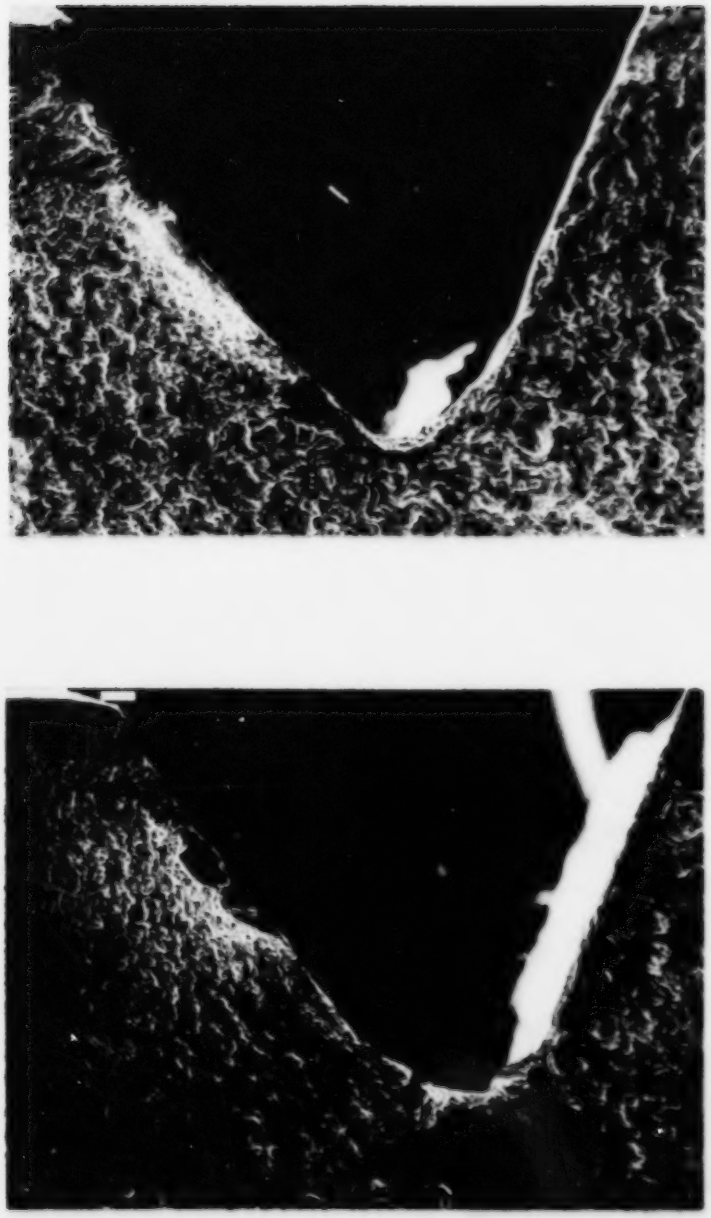

FIGURE 50 - FRACTURE SURFACES, THREADS 4 AND 6, INITIATION ZONE, X50

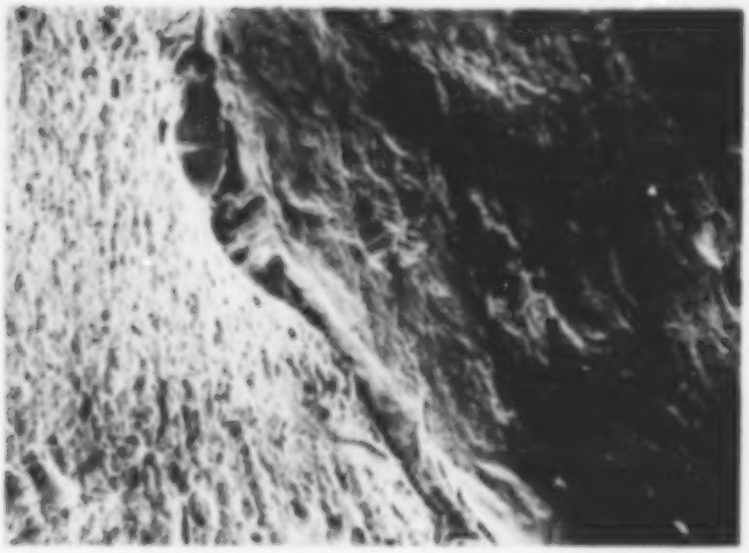

a) Fracture and thread surfaces, X100

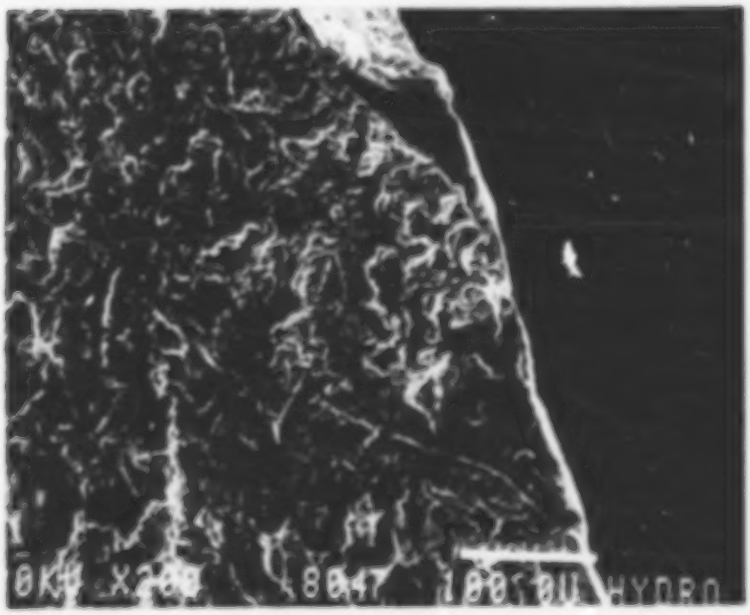

b) Fretting crack, X200

FIGURE 51 - DETAILS OF INITIATION ZONE,THREAD 6, LARGE CRACK

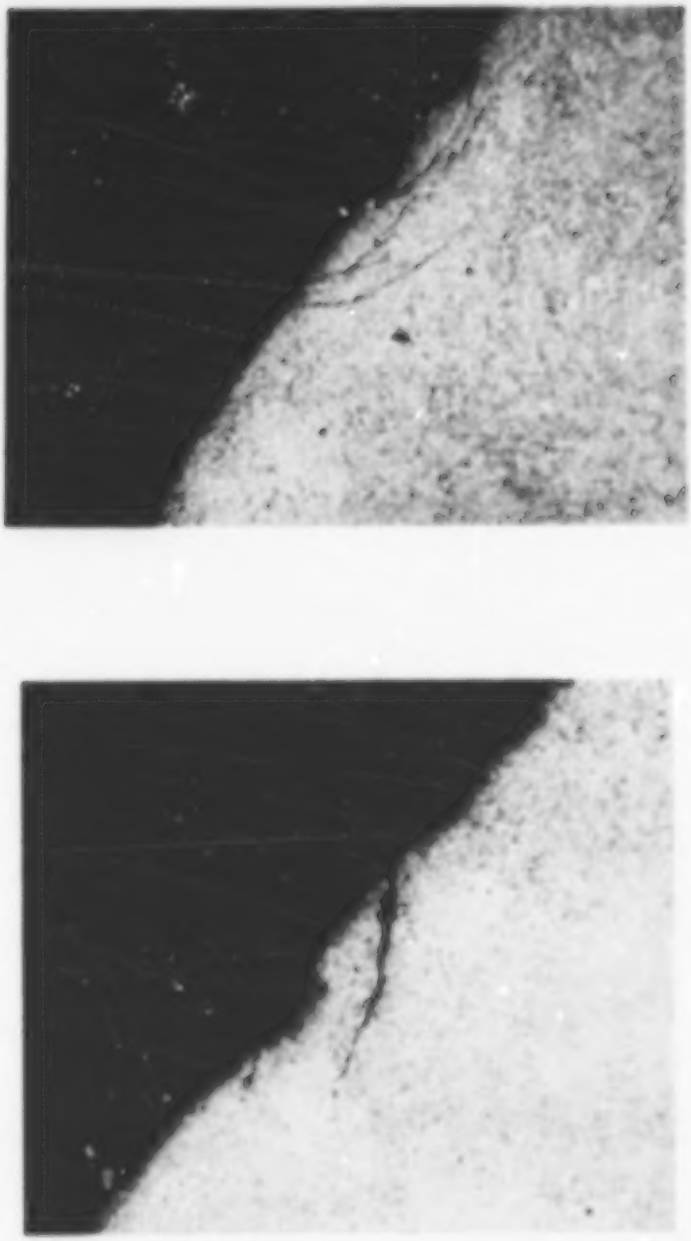

FIGURE 52 - METALLOGRAPHY OF THREAD SURFACES BEHIND LARGE CRACK, X200

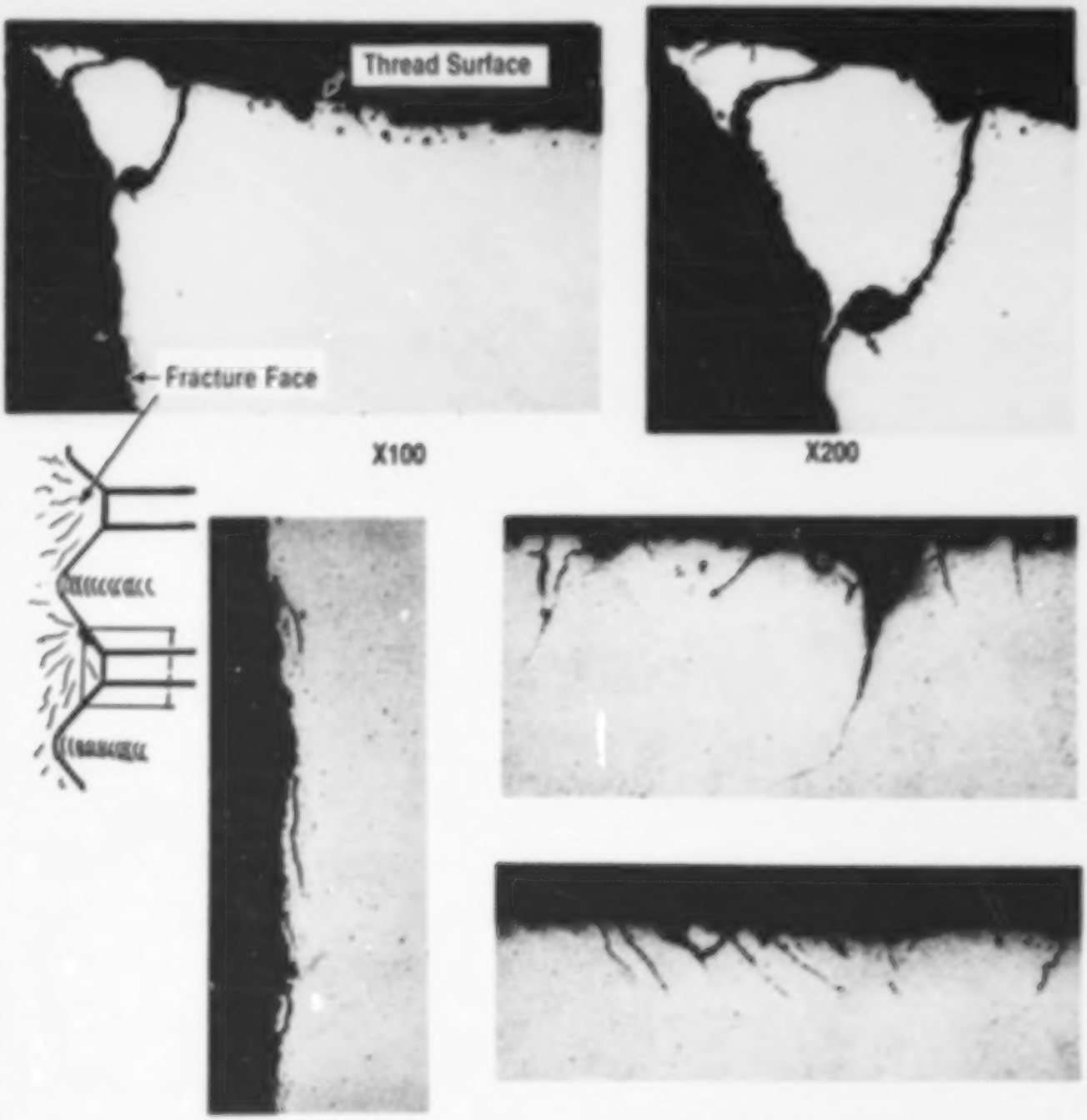

FIGURE 53 - METALLOGRAPHY OF LARGE CRACK,FRACTURE PLANE AND THREAD SURFACE, THREAD 6.

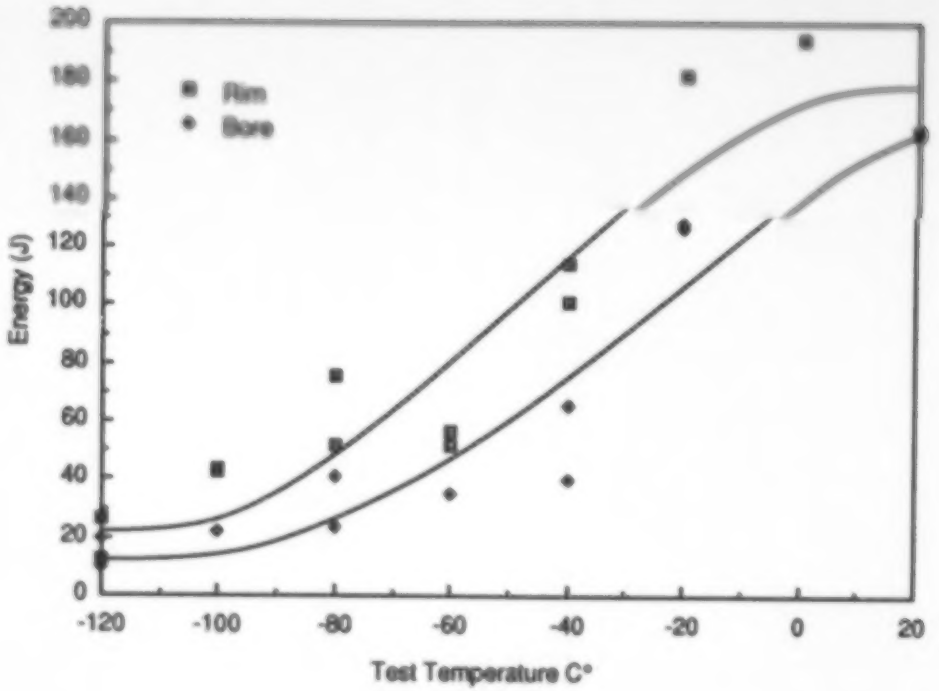

FIGURE 54

ABSORBED ENERGY VS TEMPERATURE - U2 GENERATOR SHAFT

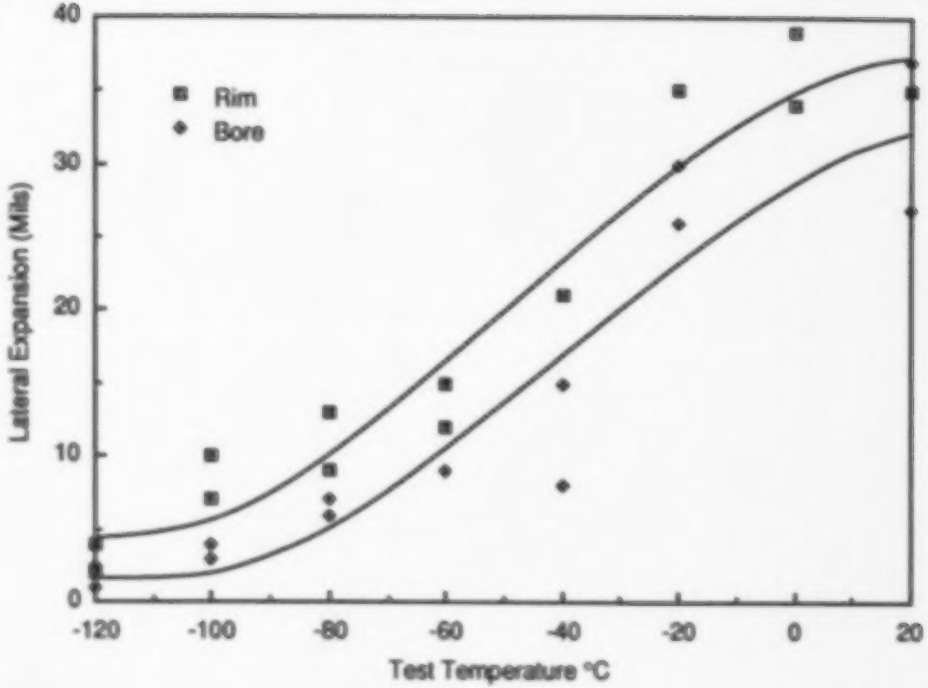

FIGURE 55

LATERAL EXPANSION VS TEMPERATURE - U2 GENERATOR SHAFT

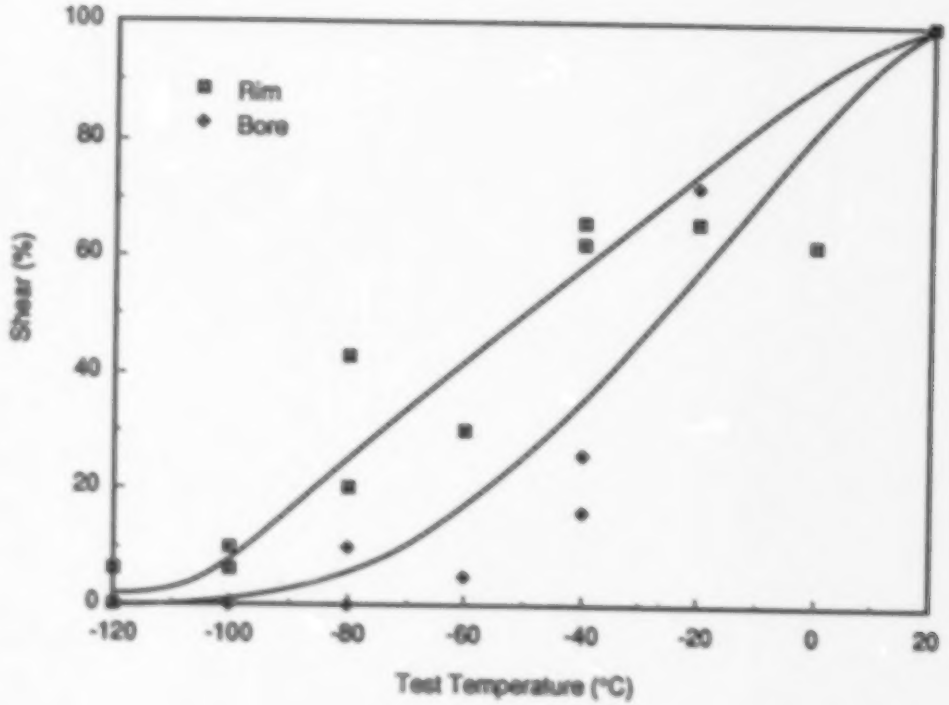

FIGURE 56

FRACTURE APPEARANCE VS TEMPERATURE - U2 GENERATOR SHAFT

TABLE 1

RESULTS OF CHEMICAL ANALYSIS
UNIT 2, GENERATOR SHAFT

(WT %, CONCENTRATION)				
ELEMENT	LOCATION			SPECIFIED VALUES (ST 577)
	RIM	MID RADIUS	BORE	
Carbon	0.25	0.24	0.23	0.22 - 0.32
Manganese	0.26	0.25	0.26	0.2 - 0.5
Silicon	0.019	0.018	0.018	0.3 Max.
Nickel	3.44	3.72	3.68	3.2 - 4.0
Chromium	1.53	1.57	1.47	1.2 - 1.8
Molybdenum	0.38	0.37	0.37	0.3 - 0.6
Vanadium	0.093	0.093	0.089	0.05 - 0.15
Phosphorus	<0.005	0.005	<0.005	0.015 Max
Sulphur	0.005	0.005	0.005	0.018 Max
Tin	0.01	0.01	0.01	NS
Antimony	0.015	0.015	0.015	NS
Arsenic	<0.02	<0.02	<0.02	NS
Copper	0.1	0.1	0.1	NS
Aluminum	0.01	0.012	0.013	NS

NS = Not Specified

TABLE 2

TENSILE PROPERTIES OF ROTOR STEEL

	UTS (MPa)	YS (MPa)	% ELONGATION	% REDUCTION OF AREA
Axial Rim	888	787	25.5	71
Axial Bore	860	764	28.0	61
Tangential Rim	893	794	22.5	60.5
Tangential Bore	855	751	24.5	68
ABB Specs. Rim	800-950	700	18/16/14	NS
Bore	NS	650	14	NS

NS = Not Specified